2009-01-0102

# Tire Models for Vehicle Dynamic Simulation and Accident Reconstruction

Raymond M. Brach, University of Notre Dame, Brach Engineering,
R. Matthew Brach, Brach Engineering



## ABSTRACT

Various vehicle dynamic simulation software programs have been developed for use in reconstructing accidents. Typically these are used to analyze and reconstruct preimpact and postimpact vehicle motion. These simulation programs range from proprietary programs to commercially available packages. While the basic theory behind these simulations is Newton's laws of motion, some component modeling techniques differ from one program to another. This is particularly true of the modeling of tire force mechanics. Since tire forces control the vehicle motion predicted by a simulation, the tire mechanics model is a critical feature in simulation use, performance and accuracy. This is particularly true for accident reconstruction applications where vehicle motions can occur over wide ranging kinematic wheel conditions. Therefore a thorough understanding of the nature of tire forces is a necessary aspect of the proper formulation and use of a vehicle dynamics program.

This paper includes a discussion of tire force terminology, tire force mechanics, the measurement and modeling of tire force components and combined tire force models currently used in simulation software for the reconstruction of accidents. The paper discusses the difference between the idealized tire force ellipse and an actual tire friction ellipse. Equations are presented for five tire force models from three different simulation programs. Each model uses a different method for computing tire forces for combined braking and steering. Some experimentally measured light vehicle tire properties are examined.

Some tire force models begin with a specified level of braking force and use the friction ellipse to determine the corresponding steering force; this produces steering forces and a resultant tire force equal in magnitude to full skidding for combined steering and braking. Comparisons are presented of results from simulation programs using different tire models for vehicle motions involving two types of severe yaw. The comparisons in this paper are not of reconstructions where the user seeks initial conditions to match an existing trajectory. The first comparison is a hypothetical postimpact motion with a given initial velocity and initial angular velocity and the other is a sudden steer maneuver. In some cases, the simulations and their tire models predict the vehicle motion closely. In most cases, however, the results differ significantly between simulation programs.

The example simulations presented in this paper are not intended to reflect the way vehicle dynamic simulation programs are used typically in accident reconstruction.

## INTRODUCTION:

Tire Models: Beside helping to provide a smooth ride, the main function of an automotive pneumatic tire is to transmit forces ($F_x$, $F_y$, $F_z$) and moments in

The Engineering Meetings Board has approved this paper for publication. It has successfully completed SAE's peer review process under the supervision of the session organizer. This process requires a minimum of three (3) reviews by industry experts.

ISSN 0148-7191

three mutually perpendicular directions for vehicle directional control. This important role of tires has made tire behavior the subject of continuous study (and performance improvement) for nearly 80 years.

Numerous tests have been conducted and mathematical models have been developed in an attempt to understand and predict the generation of these forces. These models have been divided into four different classifications [Pacejka]: 1) those that use a complex physical model, 2) those using a simple physical model, 3) models using similarity methods, and 4) models based solely on experimental data, so-called empirical models. Physical models are those intended to model tire performance (rather than vehicle performance). Physical models are concerned with such things as tire wear, temperature, traction, life, cost, etc. They have parameters such as construction, materials, loads, inflation pressure, geometry, tread design, speed, and so on. Complex physical models typically use finite element modeling techniques. Finite element models of the tires are of particular use when considering the interaction between the tire and road irregularities and for investigations into the friction between the road and the tire within the footprint of the tire [Tonuk and Unlusoy, Hölscher, et al.]. Models based on similarity methods were useful early in the tire force model development process but have found less use recently as they have been superceded by the utility afforded by other models. Such methods are covered by Pacejka [Pacejka].

The two remaining model classifications, the simple physical model and the empirical models, are the two most prevalent models used in the understanding and prediction of tire forces. They relate the physical and kinematic properties of tires to the development of tractive forces at the contact between the tire and the roadway surface. One of the most widely used simple physical models is the brush model. Brush models have been improved and developed over the recent years [Gäfvert & Svedenius] but have not yet found their way into dynamic simulation programs applied to accident reconstruction. A thorough coverage of the brush model is presented elsewhere [Pacejka].

The remaining tire model classification is the empirical tire model. Such models are also referred to as semi-empirical tire models in many references [Pacejka, Guo]. These models deal exclusively with the steady-state behavior of a tire. Treatment of the transient behavior of the tire, for example oscillatory response, response lag and wheel unbalance, is given elsewhere [Pacejka, Allen, et al.]. Empirical models employ mathematical functions capable of emulating the highly nonlinear behavior of the forces generated by the tires. These mathematical functions can range from straight line segment approximations to nonlinear functions that contain numerous coefficients based on experimental data and determined by curve-fitting routines. The principal use of these models is in the prediction of tire forces for vehicle dynamics simulation software. Many of these empirical models exist [Pacejka, Guo, Gäfvert, Hirschberg, Brach & Brach (2000), Pottinger, et al.]. This type of model is examined in this paper.

Tire forces are separated into a longitudinal force component (braking and driving) and a lateral force component (steering/cornering). The longitudinal tire force typically is mathematically expressed (modeled) and measured as a function of a variable called wheel slip. In some cases the longitudinal force is modeled simply by a prescribed force level, sometimes expressed as a fraction of the normal force. The lateral tire force is mathematically expressed (modeled) and measured as a function of a variable called the slip angle. A third, distinct, feature of a tire force model is the method of properly combining these two force components for conditions of combined braking (wheel slip) and steering (slip angle). Other forces and moments exist at the tire-road interface that are important for vehicle handling and design but are not considered here. Effects such as self-aligning torque, camber steer, conicity steer, ply steer, etc. are usually neglected for accident reconstruction applications.

Portions of this paper were presented orally at a conference [Brach & Brach, 2008].

**Vehicle Dynamic Simulation:** The use of vehicle dynamics models in the field of accident reconstruction to simulate vehicle motion has evolved steadily over the last few decades. Initially, the options of the reconstructionist were limited to the vehicle dynamics capabilities of the variants of the government-funded SMAC & HVOSM [McHenry, Segal] computer programs being the most readily available options. Even today, simulation software appears to be underutilized in the field as some reconstructionists continue to use simplified methods in attempts to address complex motion of a vehicle based on assumptions of constant deceleration [Fricke 1, Fricke 2, Orlowski, Daily, et al., Martinez] and even concepts such as point mass rotational friction [Keifer, et al. (2005)

and Keifer, et al. (2007)]. Various simulation programs currently are available to the accident reconstructionist in the form of computer-based vehicle dynamics programs and are becoming an integral part of various accident reconstruction software [PC-Crash, HVE, VCRware]. These vehicle dynamic programs were developed from within the accident reconstruction community and are particularly suited to the needs of that field. Other, more complex vehicle dynamic software is also available [VDANL, Car-Sim, ADAMS]. While the latter software can be used in accident reconstruction work, their complexity is better suited as vehicle handling models.

The basic premise behind all of the variations of vehicle dynamics simulation programs is essentially the same: the user or the software itself provides initial conditions (position, orientation, velocity) for the vehicle, the vehicle-specific geometry, the vehicle physical parameters (including tire parameters), and any time-dependent parameters (such as steering input, braking/acceleration, etc.). The program integrates the differential equations of motion of the vehicle (and semitrailer) to predict the motion as a function of time. The needs that the accident reconstruction community has for a simulation program can differ from other users of vehicle dynamics programs. Such needs include the ability to capture the dynamics of the vehicle through a wide range of motion and vehicle conditions such as damaged or altered wheelbase and/or track width, one or more wheels that are locked, large initial yaw rates of rotation following an impact, etc. In contrast, vehicle design and development work typically use vehicle dynamics to study the performance of a vehicle in its as-designed condition and operation.

Comparisons have been made [Han and Park] between EDVAP [HVE], PC-Crash [PC-Crash] and a proprietary simulation program. These comparisons consisted of three categories of initial conditions that result in three different types of postimpact motion. Category 1 uses initial conditions with a relatively high yaw velocity. The resulting vehicle motion showed that the yaw velocity decreased to near zero and the vehicle continued with a translational motion (rollout). Category 2 uses initial conditions that resulted in a nonzero yaw velocity that was maintained until rest (spinout). Category 3 uses initial conditions that result in the vehicle experiencing a moderate yaw velocity and translation. The results showed that the largest differences between EDVAP and PC-Crash occurred for the initial conditions of Category 1. Only small differences were found for Categories 2 and 3. All three tire force models use the friction ellipse to compute combined tire forces.

In all cases, the accuracy of the tire force is of considerable importance to the users of the simulation software. To a great extent, simulation accuracy depends on the ability of the tire model to predict accurately the forces acting in the plane of the roadway generated by each of the vehicle's tires. Other than aerodynamic forces, considered later in the paper, it is the tire forces acting at the tire contact patches that control the motion of the vehicle.

This paper focuses on the tire models used by three currently available simulation programs, PC-Crash, HVE and VCRware. These all have the capability to simulate motion in two dimensions. Some have more general capabilities such as three dimensional motion but these features are not considered here. The tire models used by each of these software programs is described in detail. This treatment is followed by two comparisons of simulation results using each software package for the same set of tire parameters, vehicle parameters and initial conditions. The paper concludes with a discussion of the results of the simulations. The topic of the tire friction ellipse is discussed. It is shown that the idealized friction ellipse can differ significantly from a plot of the limit of tire forces developed by actual tires.

## NOTATION, ACRONYMS AND DEFINITIONS

- **BNP:** Bakker-Nyborg-Pajecka equations (also known as the Magic Formula) [Pacejka]
- **Cornering stiffness:** see $C_\alpha$
- **Cornering compliance:** $1/C_\alpha$
- **EDSMAC4:** simulation software [HVE],
- **frictional drag coefficient, $\mu$:** average, constant value of the coefficient of friction of a tire fully sliding over a surface under given conditions (wet, dry, asphalt, concrete, gravel, ice, etc.) appropriate to an application,
- **friction circle:** the friction ellipse when $\mu_x = \mu_y$,
- **friction ellipse:** an idealized curve with coordinates consisting of the longitudinal and lateral tire force components that defines the transition of a tire from wheel slip to the condition of full sliding,
- **lateral (side, cornering, steering):** in the direction of the *y* axis of a tire's coordinate system,
- **longitudinal (forward, rearward, braking, accelerating, driving):** in the direction of the *x*

axis of a tire's coordinate system,
• **PC-Crash:** simulation software [PC-Crash],
• **SIMON: SI**mulation **MO**del **N**onlinear [HVE]
• **sliding**: the condition of a moving wheel and tire locked from rotating ($s$ = 1), or moving sideways ($\alpha$ = π/2),
• **VCRware:** simulation software [VCRware],
• $C_\alpha$: lateral tire force coefficient (also cornering coefficient),
• $C_s$: longitudinal tire force coefficient,
• $F_b$**:** input value for the braking or acceleration force, PC-Crash,
• $F_x(s)$**:** an equation with a single independent variable, $s$, that models a longitudinal tire force *for no steering, $\alpha$ = 0*,
• $F_y(\alpha)$**:** an equation with a single independent variable, $\alpha$, that models a lateral force *for no braking, s = 0*,
• $F_x(\alpha,s) = F_x[F_x(s),F_y(\alpha),\alpha,s]$**:** an equation with two independent variables, ($\alpha$,$s$), that models a longitudinal tire force component *for combined braking and steering*,
• $F_y(\alpha,s) = F_y[F_x(s),F_y(\alpha),\alpha,s]$**:** an equation of two independent variables, ($\alpha$,$s$), that models a lateral tire force component *for combined braking and steering*,
• $F_z$**:** wheel normal force,
• **full sliding**: a condition when the combined slip variables ($\alpha$,$s$) give a resultant tire force equal to $\mu F_z$, see *sliding*,
• **HVOSM: H**ighway **V**ehicle **O**bject **S**imulation **M**odel
• **m-smac:** simulation software [m-smac]
• **NCB:** Nicolas-Comstock-Brach equations [Brach & Brach 2000, 2005]
• **rollout:** translational motion alone of a vehicle that continues following spinout,
• $s$: longitudinal wheel slip,
• **slip velocity:** the velocity of the center of a tire at the contact patch relative to the ground,
• **slip angle:** $\alpha$,
• **SMAC: S**imulation **M**odel of **A**utomobile **C**ollisions [McHenry]
• **spinout:** motion of a vehicle that includes both translation and yaw rotation,
• $T$: an input value for the braking or acceleration force, SMAC,
• **wheel slip:** see $s$,
• $V_x$, $V_y$**:** components of the velocity of a wheel's hub expressed in the tire's coordinate system,
• $V_p$**:** slip velocity of a tire at point P of the tire patch.
• ***x-y-z*:** orthogonal wheel coordinates where $x$ is in the direction of the wheel's heading and $z$ is perpendicular to the tire's contact patch (see Fig 1),
• **yaw:** vehicle rotation about a vertical axis
• $\alpha$: tire slip angle (also, lateral slip angle),
• $\beta_p$**:** angle of a tire's slip velocity relative to the tire's $x$ axis and angle of the resultant force parallel to the road plane (see Fig 2),
• $\beta$**:** angle relative to the $x$ axis of the resultant tire force (see Fig 2),
• $\bar{\beta}$ **:** nondimensional slip angle, Eq 45 & 50, SMAC,
• $\mu_x$**:** tire-surface frictional drag coefficient for full sliding in the longitudinal direction, $s$ = 1, $\alpha$ = 0,
• $\mu_y$**:** tire-surface frictional drag coefficient for full sliding in the lateral direction, $\alpha$ = π/2.

## TIRE KINEMATICS

Two kinematic variables typically are used with tire force models and with the measurement of tire forces. These are the slip angle, $\alpha$, and the longitudinal wheel slip, $s$. The slip angle, is illustrated in Fig 1 and is defined as

$$\alpha = \tan^{-1}(V_y / V_x) \quad (1)$$

The wheel slip can have different definitions [Brach & Brach (2000), Pacejka]. The one used here is such that 0 ≤ $s$ ≤ 1, where

$$s = \frac{V_x - R\omega}{V_x} \quad (2)$$

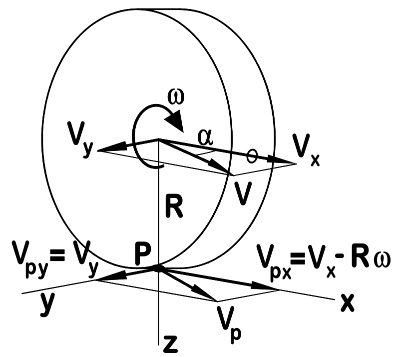

**Figure 1. Wheel/tire velocities**

Figures 1 and 2 show the tire slip velocity components $V_{Px} = V_x - R\omega$ and $V_{py} = V_y$. Note that in general the vector velocity, $V$, at the wheel hub and the slip velocity, $V_p$, at the contact patch center differ both in magnitude and direction. The slip velocity, $V_p$, is the velocity of the point P relative to the road surface. Also, the direction of the resultant force, $F$, and the slip velocity, $V_p$, can differ. For no steering, the longitudinal (braking, accelerating) tire force component, $F_x(s)$, typically is expressed mathematically as a function of the wheel slip alone.

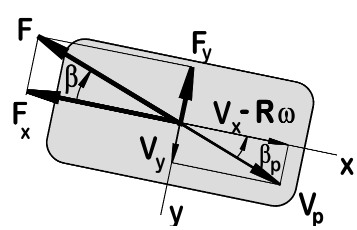

**Figure 2. Tire patch velocity and force components.**

Similarly, for no braking, the lateral (cornering, steering) force component, $F_y(\alpha)$, typically is expressed mathematically as a function of the slip angle alone.

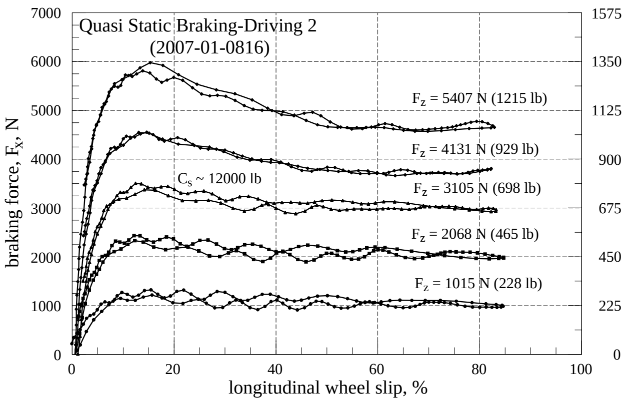


**Figure 3. Experimentally measured longitudinal tire forces, P225/60R16 tire [Salaani].**

## EXPERIMENTALLY MEASURED TIRE FORCES

Experimental tire data are presented here because some of the simulation results given later in the paper use tire parameters corresponding to measured values. The amount of data presented here is limited; more is given in a recent paper [Salaani] including a longitudinal tire force, $F_x(s)$, as a function of wheel slip, $s$, and lateral tire force, $F_y(\alpha)$, as a function of slip angle $\alpha$. Figure 3 shows $F_x(s)$ for a P225/60R16 tire for different normal forces. Figure 4 shows measured values of $F_y(\alpha)$ for different normal forces. As indicated by the notation, $F_x(s)$ is measured for zero slip angle, $\alpha$, and $F_y(\alpha)$ is measured for zero wheel slip, $s$. These tire properties are emulated later for use with a 2006 Ford Crown Victoria for which the P225/60R16 tire is standard.

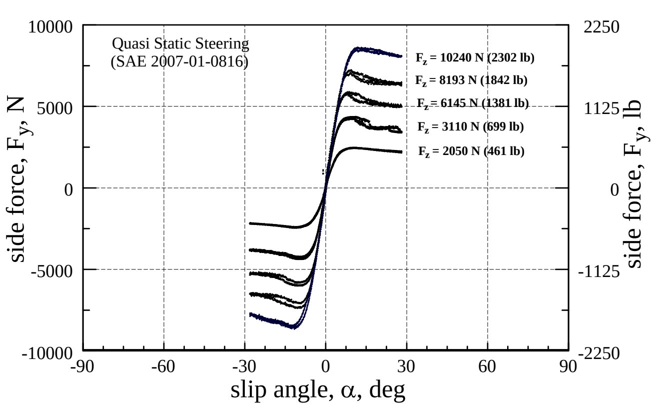


**Figure 4. Experimentally measured lateral tire forces, P225/60R16 tire [Salaani].**

From Fig 4 it can be seen that the slip coefficient, $C_\alpha$, (the slope of the initial linear portion of the curves) depends on the normal force, $F_z$. A least square fit (using the BNP equations) illustrating this dependence is shown in Fig 5. Figure 3 similarly shows that the slip stiffness coefficient, $C_s$, depends on the normal force.

## FRICTION ELLIPSE, TIRE FORCE ELLIPSE

The $x$-$y$ coordinate system and velocities of a rotating wheel are illustrated in Fig 1. The tire force components $F_x = F_x(\alpha,s)$, $F_y = F_y(\alpha,s)$ and resultant, $F = F(\alpha,s)$, are illustrated over a tire-road contact patch in Fig 2. According to the Nicolas-Comstock theory [Brach & Brach (2000)], the force components form a force ellipse where the abscissa is the longitudinal tire force component, $F_x(\alpha,s)$, and ordinate is the lateral tire force component, $F_y(\alpha,s)$. The equation of the tire force ellipse is given by Eq 3, or in a more concise form in Eq 4. The resultant force is $F(\alpha,s)=\sqrt{F_x^2(\alpha,s)+F_y^2(\alpha,s)}$.

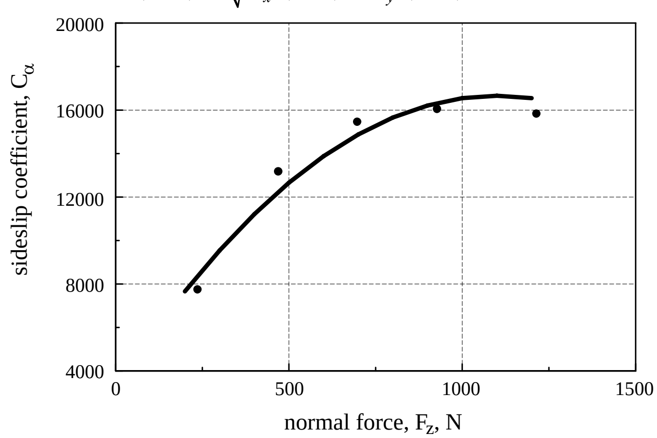


**Figure 5. Measured variation (points) of $C_\alpha$ with $F_z$, P225/60R16 tire [Salaani].**

One of the conditions of the Nicolas-Comstock tire model is that the force components are aligned with the slip velocity components, that is $\beta = \beta_p$ (Fig 2). As shown in Fig 6, the $F_x(\alpha,s)$ axis (abscissa) represents braking alone (i.e., $\alpha$ = 0). The $F_y(\alpha,s)$ axis (ordinate) represents steering alone (i.e., $s$ = 0). Each point of the friction ellipse's interior is a point with slip values ($\alpha$,$s$) for combined steering and braking that represents driver control, expressed mathematically by Eq 5. A point $F_x(s)|_{s=1} = \mu_x F_z$ on the abscissa represents locked wheel skidding for braking alone. The point, $F_y(\alpha)|_{\alpha=\pi/2} = \mu_y F_z$, on the ordinate represents a vehicle tire sliding laterally. Note that this formulation allows for different frictional drag coefficients in the $x$ and $y$ directions, $\mu_x$ and $\mu_y$, respectively. Full sliding of the tire under any combination of $\alpha$ and $s$ occurs if the

$$\frac{F_x^2\left[F_x(s),F_y(\alpha),\alpha,s\right]}{F_x^2(s)}+\frac{F_y^2\left[F_x(s),F_y(\alpha),\alpha,s\right]}{F_y^2(\alpha)}=1 \quad (3)$$

$$\frac{F_x^2(\alpha,s)}{F_x^2(s)}+\frac{F_y^2(\alpha,s)}{F_y^2(\alpha)}=1 \quad (4)$$

$$\frac{F_x^2(\alpha,s)}{\mu_x^2 F_z^2}+\frac{F_y^2(\alpha,s)}{\mu_y^2 F_z^2}<1 \quad (5)$$

$$\mu=\frac{\mu_x\mu_y}{\sqrt{\mu_x^2\sin^2\alpha+\mu_y^2\cos^2\alpha}} \quad (6)$$

resultant tire force reaches the friction ellipse, $F(\alpha,s) = \mu F_z$, where the frictional drag coefficient, $\mu$ is given by Eq 6 [Brach & Brach (2000)]. For a given normal force, $F_z$, points outside the Friction Ellipse cannot be reached because the friction force is limited by $\mu F_z$. If $\mu_x = \mu_y$, then the tire force ellipse becomes a circle and the friction ellipse becomes a friction circle.

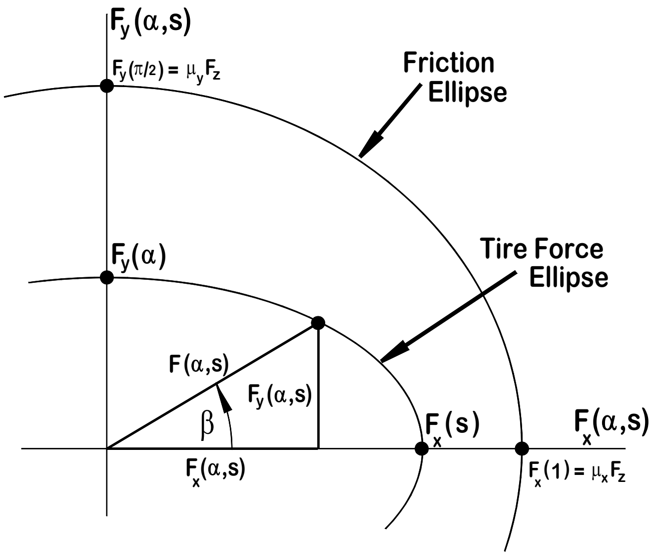


**Figure 6. Diagrams of Friction (Limit) Ellipse and Tire Force Ellipse.**

Model equations that determine the functions $F_x(\alpha,s)$ and $F_y(\alpha,s)$ for combined steering and braking (such as shown in Fig 6 as a tire force ellipse) must be found independently from the steering and braking functions $F_y(\alpha)$ and $F_x(s)$. This is done later. It is important to note that the friction ellipse is not a tire model. Rather, it is an idealized graphical display of the operating limit for resultant tire forces for any combination of steering and braking. More than one method exists for developing the resultant tire force for combined steering and braking. One is shown in the next Section; others are [Pottinger, et al. and Schuring, et al.] and [Hirschberg].

## SIMULATION TIRE MODELS

Different tire force models exist and at least one survey has been written [Gäfvert, M. and J. Svedenius], but the equations of most commonly used models are not cataloged. The following is a collection of the equations of tire force models used in three vehicle dynamics simulation software packages used for reconstructing accidents.

**VCRware Tire Model:** The longitudinal and lateral tire force equations for this simulation software are modeled using a subset of the BNP equations [Pacejka]. Equation 7 gives the longitudinal force, $F_x(s)$, for braking alone with no steering ($\alpha$ = 0). Figure 7 shows an example of a normalized plot of the longitudinal tire force with example BNP parameter values of $B$ = 1/15, $C$ = 1.5, $D$ = 1.0, $E$ = 0.30, $K$ = 100.0 and where the initial slope is the braking coefficient $C_s = BCDK$.

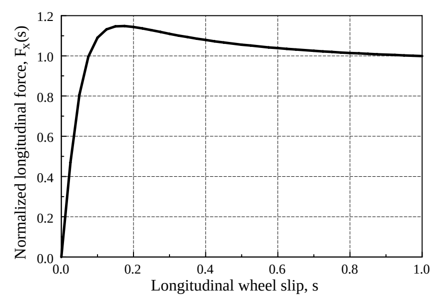


**Figure 7. BNP longitudinal force as a function of wheel slip, *s*, VCRware.**

Equation 8 gives the lateral steering force, $F_y(\alpha)$, for no braking ($s$ = 0). Figure 8 shows a sample normalized lateral force with BNP parameter values of $B$ = 8/75, $C$ = 1.5, $D$ = 1.0, $E$ = 0.60, $K$ = 100.0 and the lateral stiffness coefficient is $C_\alpha = BCDK$.

For a wheel with a braking force, $F_x(s)$, and a lateral force, $F_y(\alpha)$, the longitudinal force for combined steering and braking, $F_x(\alpha,s)$, is determined in VCRware using the Nicolas-Comstock-Brach, (NCB) equations [Brach & Brach (2000) and Brach & Brach (2005)]. It is given by Eq 9. For a wheel with a braking force, $F_x(s)$, and a lateral force, $F_y(\alpha)$, the lateral force for combined steering and braking, $F_y(\alpha,s)$, is determined using the NCB equation and is given by Eq 10.

$$F_x(s) = D\sin\left\{C\tan^{-1}\left[B(1-E)Ks + E\tan^{-1}(BKs)\right]\right\} \tag{7}$$

$$F_y(\alpha) = D\sin\left\{C\tan^{-1}\left[B(1-E)K\frac{2\alpha}{\pi} + E\tan^{-1}(BK\frac{2\alpha}{\pi})\right]\right\} \tag{8}$$

$$F_x(\alpha,s) = \frac{F_x(s)F_y(\alpha)s}{\sqrt{s^2F_y^2(\alpha)+F_x^2(s)\tan^2\alpha}}\frac{\sqrt{s^2C_a^2+(1-s)^2\cos^2\alpha F_x^2(s)}}{sC_\alpha} \tag{9}$$

$$F_y(\alpha,s) = \frac{F_x(s)F_y(\alpha)\tan\alpha}{\sqrt{s^2F_y^2(\alpha)+F_x^2(s)\tan^2\alpha}}\frac{\sqrt{(1-s)^2\cos^2\alpha F_y^2(\alpha)+C_s^2\sin^2\alpha}}{C_s\sin\alpha} \tag{10}$$

When plotted on axes of $F_x(s)$ and $F_y(\alpha)$, the NCB equations take the form of a tire force ellipse that depends on the functions $F_x(s)$ and $F_y(\alpha)$. Three-dimensional surface plots of these combined tire forces are illustrated in Appendix A.

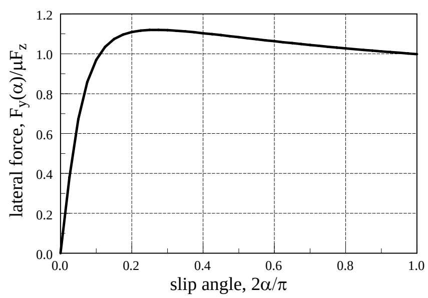


**Figure 8. BNP lateral tire force as a function of normalized slip angle, $2\alpha/\pi$, VCRware.**

**PC-Crash Linear Tire Force Model:** PC-Crash allows the choice of either of two tire models, the Linear Tire Force model and the TM-Easy Tire Force model. The Linear Tire model is as follows.

Instead of using the wheel slip parameter, $s$, the PC-Crash simulation requires an input value of a constant magnitude of applied braking force with a force level, $F_b$, or an acceleration force magnitude, $F_a$. A force specified as a fraction of the wheel normal force can alternatively be supplied. For no steering the longitudinal accelerating force, is specified as $F_x = F_a$, and the longitudinal braking force is $F_x = -F_b$. The PC-Crash vehicle dynamic simulation uses a bilinear lateral tire force as shown in Fig 9. The linear portion represents a slip coefficient of $C_\alpha$.

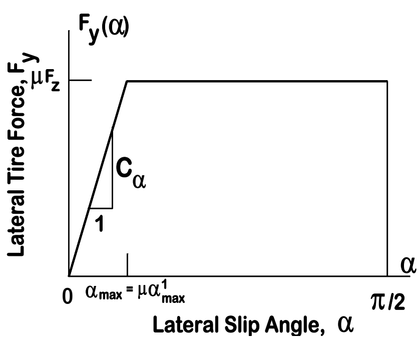


**Figure 9. Lateral tire force, Linear Tire Model, PC-Crash.**

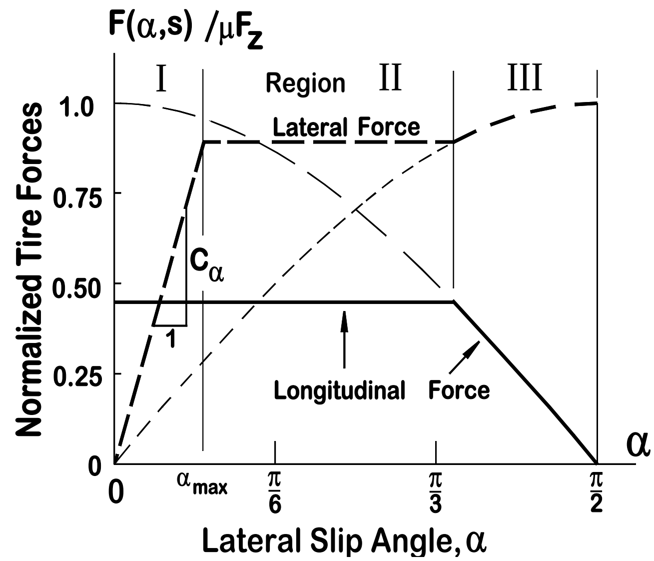


**Figure 10. Diagram of the longitudinal and lateral tire forces, PC-Crash Linear Tire Model.**

The lateral force becomes constant at $\alpha = \alpha_{max}$, where the lateral force reaches its maximum value $\mu F_z$. For the PC-Crash protocol, $\alpha_{max} = \mu\alpha^1_{max}$, where $\alpha^1_{max}$ is the saturation angle for $\mu_y = 1$. For this notation, the tire slip coefficient is computed as $C_\alpha = \mu F_z/\alpha^1_{max}$. For no longitudinal force, $s = 0$, ($F_a = F_b = F_x = 0$) the lateral tire force is defined by Eq 11 and 12. For a wheel with braking force $F_x(\alpha,s) = F_b$ the lateral force is computed using the friction ellipse as given in Eq 13 where the longitudinal force is adjusted for the condition of locked wheel skidding as shown in Eq 14. For combined steering and braking, the PC-Crash Linear Tire Model can be described in three regions (see Fig 10). Region I is when the side force increases linearly with $\alpha$, Eq 15. Region II is when the side force is said to be saturated and the lateral force is computed using the friction ellipse, Eq 16 and Region III is for locked wheel sliding, as shown in Eq 17.

$0 \le \alpha \le \alpha_{max} = \mu\alpha^{1}_{max}$: $F_y(\alpha) = -\mu F_z \alpha / \mu\alpha^{1}_{\max}$ (11)

$\alpha_{max} < \alpha < \pi/2$: $F_y(\alpha) = \mu F_z$ (12)

$$F_y(\alpha, s) = \min\left[\mu F_z \frac{\alpha}{\alpha_{\max}}, \sqrt{(\mu F_z)^2 - F_x^2(\alpha, s)}\right] \quad (13)$$

$$F_x(\alpha, s) = \min\left[F_b, \mu F_z \cos\alpha\right] \quad (14)$$

$$F_y(\alpha, s) = \mu F_z \frac{\alpha}{\alpha_{\max}} \quad (15)$$

$$F_y(\alpha, s) = \sqrt{(\mu F_z)^2 - F_b^2} \quad (16)$$

$$F_y(\alpha, s) = \mu F_z \sin\alpha \quad (17)$$

$$\sqrt{F_y^2(\alpha, s) + F_b^2} = \mu F_z \quad (18)$$

These regions are shown in Fig 10 and are plotted on the friction ellipse in Fig 11. As the slip angle, $\alpha$, increases from 0 to $\alpha_{max}$, $F_y(\alpha,s)$ goes from (0,0) to point A. The magnitude of the lateral force, $F_y(\alpha,s)$, at point A is determined by $F_b$ and Eq 17. Note that in Region II, while the slip angle increases from $\alpha_{max}$ to some value greater than $\alpha_{max}$ as shown in Fig 10, the resultant force at the patch does not change. Thus Region II, for which $\alpha$ varies from $\alpha_{max}$ to some value greater than $\alpha_{max}$, is concentrated at a single point, B, on the tireforce diagram in Fig 11. In Region III $F_y(\alpha,s)$goes from point B to point C (as $\alpha$ continues to increase) along the friction circle. From Eq 17 note that for Region II (point B), Eq 18 holds. All of this implies that throughout Region II the PC-Crash Linear tire force model gives a lateral force at the friction limit on the idealized friction limit circle. Although the direction of $F_y(\alpha,s)$ is along the slip direction, the magnitude of the resultant tire force is equal to a fully skidding tire, $\mu F_z$. A surface plot of $F_y(\alpha,s)$ is given in Appendix A.

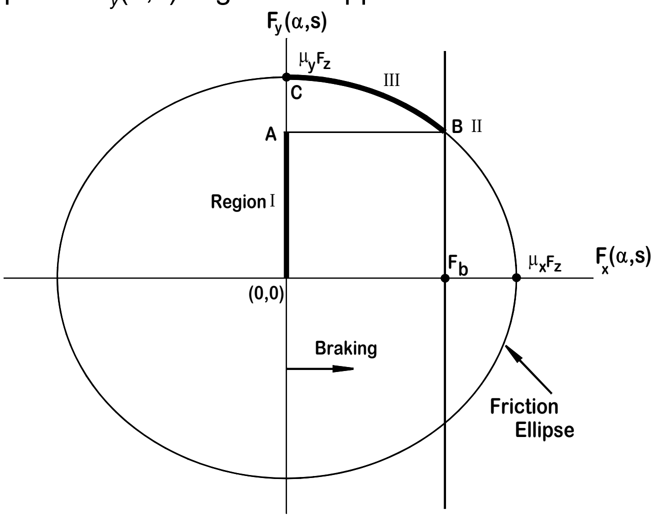


**Figure 11. Diagram of lateral and longitudinal tire forces for combined steering and braking, PC-Crash.**

**TM-Easy Tire Model [Hirschburg, et al.]:** The TM-Easy model is defined for three dimensional vehicle motion. However all of the following discussion is for zero camber and negligible contact moments. According to notes on vehicle dynamics [Rill] TM-Easy defines longitudinal slip and lateral slip different than above. Longitudinal slip, $s_x$, is defined as in Eq 19. TM-Easy lateral slip is defined as in Eq 20. The consequences of normalizing slip to the wheel angular velocity is for TM-Easy that $0 \le s_x \le \infty$, $0 \le s_y \le \infty$ and (for combined steering and braking) that $s_x$ and $s_y$ are coupled to $s$ (as defined by Eq 2) and $\alpha$ (Eq 1), as given in Eq 21 through 25. The TM-easy model specifies that beyond a certain, finite value of slip $s_{xf}$, full sliding occurs. The model can characterize a maximum longitudinal force by specifying maximum values of the force with its corresponding slip ($s_{xm}$, $F_{xm}$). Figure 12 shows the longitudinal force $F_x$ as a function of the longitudinal slip $s_x$. A full description of the model requires that three pieces of information be provided to define the shape of the $F_x(s_x)$ curve: an initial slope, $C_x$, the maximum value of the force and its associated slip value ($s_{xm}$, $F_{xm}$), and the value of the force at full sliding and its associated slip value ($s_{xf}$, $F_{xf}$). The curve for the lateral force, $F_y(s_y)$, can similarly be defined using slope, $C_y$, maximum parameters ($s_{ym}$, $F_{ym}$) and full-sliding parameters ($s_{yf}$, $F_{yf}$).

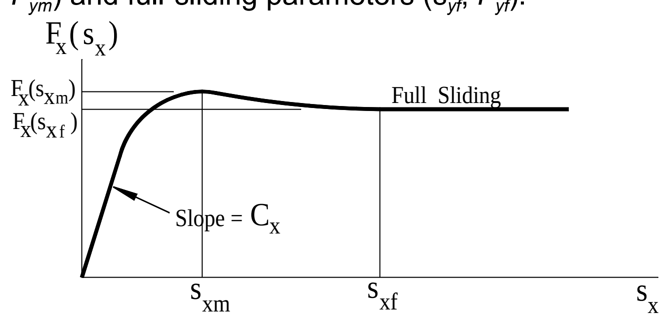


**Figure 12. Longitudinal tire force, TM-Easy model.**

The process outlined above defines the shape of the curve for the longitudinal force in the absence of lateral slip, $F_x(s_x)$, and the curve for the lateral force in the absence of longitudinal slip, $F_y(s_y)$. The force for combined braking and steering,

$$s_x = \frac{V_{px}}{R\omega} \quad (19)$$

$$s_y = \frac{V_y}{R\omega} \quad (20)$$

$$s(s_x, s_y) = \frac{V_{px}}{V_x} = \frac{V_x - R\omega}{V_x} \quad (21)$$

$$s(s_x, s_y) = 1 - \frac{R\omega}{V_{px} + R\omega} = \frac{R\omega}{s_x R\omega + R\omega} = \frac{s_x}{1 + s_x} \quad (22)$$

$$\alpha(s_x, s_y) = \tan^{-1}\left(\frac{v_y}{v_x + R\omega}\right) = \tan^{-1}\left(\frac{s_y}{1 + s_x}\right) \quad (23)$$

$$s_x(s, \alpha) = \frac{s}{1 - s} \quad (24)$$

$$s_y(s, \alpha) = \frac{\tan\alpha}{1 - s} \quad (25)$$

$$s_{xy} = \sqrt{\left(\frac{s_x}{\hat{s}_x}\right)^2 + \left(\frac{s_y}{\hat{s}_y}\right)^2} \quad (26)$$

$$\hat{s}_x = \frac{s_{xm}}{s_{xm} + s_{ym}} + \frac{F_{xm}/C_x}{F_{xm}/C_x + F_{ym}/C_y} \quad (27)$$

$$\hat{s}_y = \frac{s_{ym}}{s_{xm} + s_{ym}} + \frac{F_{ym}/C_y}{F_{xm}/C_x + F_{ym}/C_y} \quad (28)$$

$$C = \sqrt{\left(C_x \hat{s}_x \cos\varphi\right)^2 + \left(C_y \hat{s}_y \sin\varphi\right)^2} \quad (29)$$

$$s_m = \sqrt{\left(\frac{s_{xm}}{\hat{s}_m}\cos\varphi\right)^2 + \left(\frac{s_{ym}}{\hat{s}_m}\sin\varphi\right)^2} \quad (30)$$

$$F_m = \sqrt{\left(F_{xm}\cos\varphi\right)^2 + \left(F_{ym}\sin\varphi\right)^2} \quad (31)$$

$$s_f = \sqrt{\left(\frac{s_{fx}}{\hat{s}_x}\cos\varphi\right)^2 + \left(\frac{s_{fy}}{\hat{s}_y}\sin\varphi\right)^2} \quad (32)$$

$$F_f = \sqrt{\left(F_{xf}\cos\varphi\right)^2 + \left(F_{yf}\sin\varphi\right)^2} \quad (33)$$

$$\cos\varphi = \frac{s_x/\hat{s}_x}{s_{xy}} \quad \text{and} \quad \sin\varphi = \frac{s_y/\hat{s}_y}{s_{xy}} \quad (34)$$

$$F(s_x, s_y) = \frac{\sigma s_m C}{1 + \sigma\left(\sigma + F_f \frac{s_m}{F_m} - 2\right)}, \quad \sigma = \frac{s_{xy}}{s_m}, \quad 0 \le s_{xy} \le s_m \quad (35)$$

$$F(s_x, s_y) = F_m - (F_m - F_f)\sigma^2(3 - 2\sigma), \quad \sigma = \frac{s_{xy} - s_m}{s_f - s_m}, \quad s_m \le s_{xy} \le s_f \quad (36)$$

$$F(s_x, s_y) = F_f, \; s_{xy} > s_f \quad (37)$$

$$F_x(s_x, s_y) = F(s_x, s_y)\cos\varphi \quad (38)$$

$$F_y(s_x, s_y) = F(s_x, s_y)\sin\varphi \quad (39)$$

$F(s_x,s_y)$, is formulated by the TM-Easy model through the following process. A generalized slip variable, $s_{xy}$, which treats the longitudinal and lateral slip vectorially, is defined by Eq 26 where quantities $\hat{s}_x$ and $\hat{s}_y$ are normalized slip variables and are defined by Eq 27 and 28. Equations 29 through 33 define additional parameters. A generalized tire force, $F(s_x,s_y)$ is now described in each of the three intervals by a broken rational function, a cubic polynomial and a constant $F_f$ and given in Eq 35, 36 and 37. Finally, the longitudinal and lateral force components, Eq 38 and 39, are determined individually from the projections in the longitudinal and lateral directions, using $\varphi$, given by Eq 34. Three-dimensional surface plots of the longitudinal and lateral tire forces for combined steering and braking for the TM-Easy model are given in Appendix A.

**SMAC Tire Model [HVE and m-smac]:** For braking, SMAC does not use the wheel slip variable, $s$, but the simulation user is asked to specify the value of a constant braking force, $T$, which also can be defined as a percentage of the available friction force at each wheel. The longitudinal tire force, $F_x$, is given by Eq 40 through 44 for the different variations of braking and acceleration.

For braking:

$$T = 0 \; (s = 0), \quad F_x(T) = 0 \quad (40)$$

$$0 < T \le \mu F_z, \quad F_x(T) = -T \quad (41)$$

$$T > \mu F_z, \quad F_x(T) = -\mu F_z \quad (42)$$

For acceleration

$|T| \leq \mu F_z, \quad F_x(T) = T$ (43)

$|T| > \mu F_z, \quad F_x(T) = \mu F_z$ (44)

$$\bar{\beta} = \bar{\beta}(\alpha) = \frac{C_\alpha \alpha}{\sqrt{\mu^2 F_z^2}} \quad (45)$$

For $\left|\bar{\beta}\right| < 3$, $F_y(\alpha) = \mu F_z \left[\bar{\beta} - \frac{\bar{\beta}\left|\bar{\beta}\right|}{3} + \frac{\bar{\beta}^3}{27}\right]$ (46)

For $\left|\bar{\beta}\right| \geq 3$, $F_y(\alpha) = \mu F_z$ (47)

For the lateral force, SMAC uses a nondimensional variable $\bar{\beta}$, Eq 45, based on the Fiala tire model [EDSMAC, Brach & Brach (2005)] and defines the lateral force $F_y(\alpha)$ by Eq 46 and 47. $F_y(\alpha)$ is plotted in Fig 13 for typical values of $C_\alpha / \mu F_z$.

For a wheel simultaneously steered ($\alpha > 0$) and braked ($T > 0$) the longitudinal tire force, $F_x(\alpha,s)$, is computed by Eq 48 or 49, where the latter case corresponds to locked wheel skidding. For combined braking and steering, the lateral tire force, $F_y(\alpha,s)$, is computed using the longitudinal force, $\bar{\beta}$, newly defined by Eq 50 and the friction ellipse. Then for $\bar{\beta}$, Eq 51 or 52 give $F_y(\alpha,s)$. Equation 52 implies that for $\left|\bar{\beta}\right| \geq 3$ the resultant tire force lies on the friction ellipse, as given by Eq 53 and that the SMAC tire force model gives a lateral force at the friction limit for combined steering and braking (before locked wheel sliding occurs). Although the direction of the lateral force, $F_y(\alpha,s)$, is along the slip direction, the magnitude of the resultant tire force equals that of a fully skidding tire. A three-dimensional surface plot of $F_y(\alpha,s)$ using Eq 51 through 53 is included in Appendix A.

For $F_x(T) \leq \mu F_z \cos\alpha$, $F_x(\alpha,s) = T$ (48)

For $F_x(T) > \mu F_z \cos\alpha$, $F_x(\alpha,s) = \mu F_z \cos\alpha$ (49)

$$\bar{\beta} = \bar{\beta}(\alpha) = \frac{C_\alpha \alpha}{\sqrt{\mu^2 F_z^2 - F_x^2(\alpha,s)}} \quad (50)$$

For $\left|\bar{\beta}\right| < 3$,

$$F_y(\alpha,s) = \sqrt{\mu^2 F_z^2 - F_x^2(\alpha,s)}\left(\bar{\beta} - \frac{1}{3}\bar{\beta}\left|\bar{\beta}\right| + \frac{1}{27}\bar{\beta}^3\right) \quad (51)$$

For $\left|\bar{\beta}\right| \geq 3$,

$$F_y(\alpha,s) = \sqrt{\mu^2 F_z^2 - F_x^2(\alpha,s)} \quad (52)$$

$$\sqrt{F_x^2(\alpha,s) + F_y^2(\alpha,s)} = \mu F_z \quad (53)$$

**SIMON Tire Model [HVE]:** SIMON [EDC] uses a semiempirical tire model which is based upon the HSRI tire model [McAdam, et al.]. The principle behind the HSRI tire model is that the tire forms a rectangular contact patch which can be divided into two regions consisting of a no-slip region and a sliding region. The relative size of the two regions is dependant upon the longitudinal and lateral slip values, $s$ and $\alpha$, the sliding frictional drag coefficient, $\mu$, and the initial slopes, $C_s$ and $C_\alpha$, of the linear tire force curves.

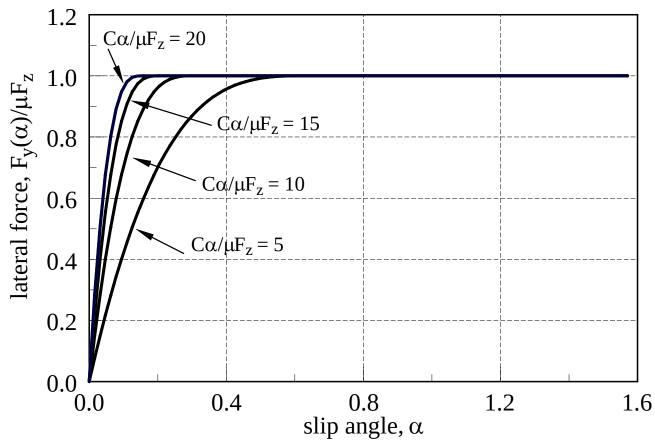


**Figure 13. Lateral tire force as a function of slip angle, *α*, SMAC.**

The first step in determining the SIMON tire forces is to determine an equivalent frictional drag coefficient, $\mu'$, that depends on the slip, $s$, and is calculated from the directional sliding frictional drag coefficients, $\mu_x$ and $\mu_y$. The coefficient $\mu'$ is found using a fitting procedure whereby,

$$a = (1 - s_p)^2 (1 + s_p) \quad (54)$$

$$b = (1 - s_p)\left(\mu_x (s_p + 2) - \mu_p (2 s_p + 1)\right) \quad (55)$$

$$c = (\mu_x - \mu_p)\mu_x \quad (56)$$

$$B = \frac{-b + \sqrt{b^2 - 4ac}}{2a} \quad (57)$$

$$A = \mu_x + B \quad (58)$$

$$C = \mu_x + B(1 - s_p) \quad (59)$$

and

$$\mu' = A - Bs \quad (60)$$

In these equations, $\mu_p$ is the ratio of longitudinal tire force $F_x(s)_{max}/F_z$ and $s_p$ is the slip at $F_x = F_x(s)_{max}$. A variable $D_t$ is defined as,

$$D_t = \sqrt{(C_s s)^2 + (C_\alpha \sin\alpha)^2} \quad (61)$$

where $s$ is the longitudinal tire slip and $\alpha$ is the slip angle. After calculating $\mu'$, a fraction, $X_s/L$, representing the portion of the total contact patch that is not slipping, where $L$ is the total length of the rectangular tire patch, is defined as:

$$\frac{X_s}{L} = \frac{\mu' F_z}{2D_t}(1-|s|),\ 0 \le \frac{X_s}{L} \le 1 \qquad (62)$$

The equations for combined steering and braking/acceleration follow. The equations for steering alone and braking alone can be found by substituting $s$ = 0 and $\alpha$ = 0 into the equations, respectively. For combined braking and steering, $X_s/L = 1$:

$$F_x(\alpha, s) = C_s \frac{s}{1-|s|} \qquad (63)$$

$$F_y(\alpha, s) = -\frac{C_\alpha \sin\alpha}{1-|s|} \qquad (64)$$

Three-dimensional surface plots of $F_x(\alpha,s)$ and $F_x(\alpha,s)$ are included in Appendix A. The sine functions in the range $-\pi \le \alpha \le \pi$ as used in the above equations for the SIMON model were changed from the tangent functions found in the original HSRI model. EDC is now investigating the full effects of this change. In addition, various empirical curves from measured tire parameters arebuilt into the HVE software that make the tire characteristics tire specific and functions of load and speed. However, the user has the ability to enter other tire characteristics or to use setup tables based upon a specific tire tests. The SIMON tire model also considers the effects that camber stiffness has on the lateral tire forces.

## SIMULATION COMPARISONS

**Comparison of Simulation Tire Force Models:** Tire forces for combined steering and braking can be compared visually using three-dimensional force plots. Plots are given for all of the different models in Appendix A.

**Computer Vehicle Dynamic Simulation**: Two examples are presented for comparison of the simulations and tire models. The first is a hypothetical, postimpact trajectory of a 2006 Ford Crown Victoria. This example is examined for three different sets of wheel conditions: A, locked wheels, B, partial drag on each wheel with a single locked front wheel and C, partial drag on each wheel. Results of the different simulations and tire models are compared on a relative basis.

The second example is for a sudden steer maneuver of a partially braked vehicle based on a test [Cliff, et al.]. Relative comparisons between the different simulation results are made. The example is intended to reflect a relatively rapid severe steer with partial braking. All of the simulations use identical vehicle and tire input data and a frictional drag coefficient of $f$ = 0.75. All input data are listed in Appendix B. These examples are intended to illustrate that uncertainty of simulations exists. Such uncertainty depends on differences in the individual characteristics of each simulation program as well as differences in the tire models. The simulation software packages used are HVE, PC-Crash and VCRware.

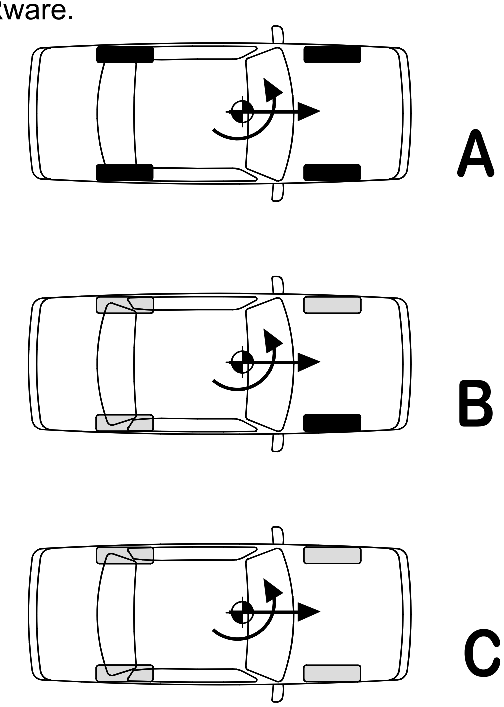


**Figure 14. Diagram of three cases A, B and C. Arrows indicate initial velocities. Gray tires indicate partial drag; black tires indicate locked wheels.**

<u>First Example (Crown Victoria)</u> The same vehicle and tire properties are used to compute the output of the different simulations for a postimpact maneuver with specified initial conditions. The vehicle corresponds to a 2006 Ford Crown Victoria. A major reason this vehicle is chosen is because it uses P225/60R16 tires with known, measured lateral steering properties [Salaani] presented earlier. The specifications of the vehicle are contained in Appendix B.

Vehicle trajectories are computed for an initial forward speed of 34.1 mph (55 km/hr), an initial lateral speed of zero and an initial yaw angular velocity of 150 °/s. Each trajectory is computed for three conditions of braking. First, the output of the simulations is compared for a case which is independent of the tire force models, that of locked wheel skidding, indicated as A in Fig 14. Then comparisons are made for the same initial conditions for equal powertrain drag on each rear

$\underline{X_s /L < 1}$:

$$F_X(\alpha,s) = C_S s\left(\frac{\mu' F_Z}{2D_t}\right)^2 (1-|s|) + \mu' F_Z\left(1-\frac{X_S}{L}\right)\left(\frac{s}{\sqrt{s^2+\sin^2\alpha}}\right) \tag{65}$$

$$F_y(\alpha,s) = -C_\alpha \sin\alpha\left(\frac{\mu' F_Z}{2D_t}\right)^2 (1-|s|) - \mu' F_Z\left(1-\frac{X_S}{L}\right)\left(\frac{\sin\alpha}{\sqrt{s^2+\sin^2\alpha}}\right) \tag{66}$$

wheel (10% of the static normal force), rolling drag on the left front wheel (0.7% of the static normal force) and a locked right front wheel, B in Fig 14. The third case is for equal powertrain drag on each rear wheels (10% of the static normal force) and equal tire rolling drag on each front wheel (0.7% of the static normal force), C in Fig 14. The results are as follows.

A. Postimpact Motion, Locked Wheel Skidding Table 1 lists the results of the locked wheel skid simulations. All three software packages and all three tire models give reasonably close rest positions, orientations and times to rest.

B. Postimpact Motion, No Applied Braking, Power Train Drag and One Locked Front Wheel For the conditions of 0.7% rolling wheel drag on the left front wheel, 10% powertrain drag on both rear wheels and the right front wheel locked, the agreement between all tire models is good, but not as close as the locked wheel condition. Table 2 lists the CG rest positions, orientations and travel times. Initial motion is in the *x* direction and lateral travel is small. VCRware and EDSMAC4 give a negative lateral travel, while PC-Crash gives a small positive travel. The times to reach the rest positions are close but not the same.

C. Postimpact Motion, No Applied Braking with Power Train Drag and Tire Rolling Resistance Results are contained in Table 3 for the same conditions as the previous case, except with rolling drag on both front wheels (no locked wheel) and for an additional tire model. Large differences in the rest positions, orientations and travel times occur. The motion in this case can be divided into two components. The first is a combination of translation and yaw rotation (spinout). At a point in the travel to rest, the yaw velocity goes to zero ($\dot{\theta} = 0$); the motion that follows consists of translation alone, or rollout, to a rest position. This is illustrated in Fig 15 for simulations using EDSMAC4, VCRware and PC-Crash (two tire models). The positions and orientations at the end of spinout differ; in particular, the angular positions are quite different. This leads to large differences in the rest positions. For reference, the locked wheel skid trajectories from the same initial conditions are shown in the same figure (note that the different rest positions are so close that only one is shown).

Note that a sensitivity analysis to changes in initial conditions was not carried out.

**Second Example (Honda Accord):** These simulations use a 1991 Honda Accord with an

initial speed of 100 km/hr (91.13 ft/s). The driver makes a sudden, constant front wheel steer maneuver to the right of approximately 9° following brake activation that causes a constant, equivalent, longitudinal deceleration of 0.273 ± 0.003 g's. The vehicle then moves to rest. Details of the input vehicle and tire data are given in Appendix C.

Since the initial vehicle speed is relatively high, simulations were run with and without aerodynamic drag where possible and, for comparison, ignoring aerodynamic drag. The aerodynamic drag force, $R_A$, in VCRware is calculated using the well known equation [Hoerner]

$$R_A = \frac{1}{2}\rho C_d A V^2 \tag{67}$$

The drag force depends on the density of air, $\rho$, a dimensionless drag coefficient, $C_d$, a projected area $A$, and a velocity relative to the wind, $V$. In all cases treated here a wind speed of zero is used. The aerodynamic drag is a resultant force calculated using frontal and lateral components. A frontal drag coefficient for all simulations had a value of $C_{dF}$ = 0.4 with a frontal area of $A_F$ = 25 ft$^2$ (2.3 m$^2$). The corresponding lateral or side values are $C_{dL}$ = 0.8 and $A_L$ = 60 ft$^2$ (5.6 m$^2$). For no aerodynamic drag $C_{dF}$ = $C_{dL}$ = 0. In some cases, an aerodynamic moment (usually small) is developed since the side force is not aligned with the vehicle center of gravity. When included, a moment arm of 0.76 ft to the rear of the CG was used.

The front and rear tire side force coefficients, $C_{\alpha f}$ and $C_{\alpha r}$, are included as input parameters in all simulations. Stock tire size on a

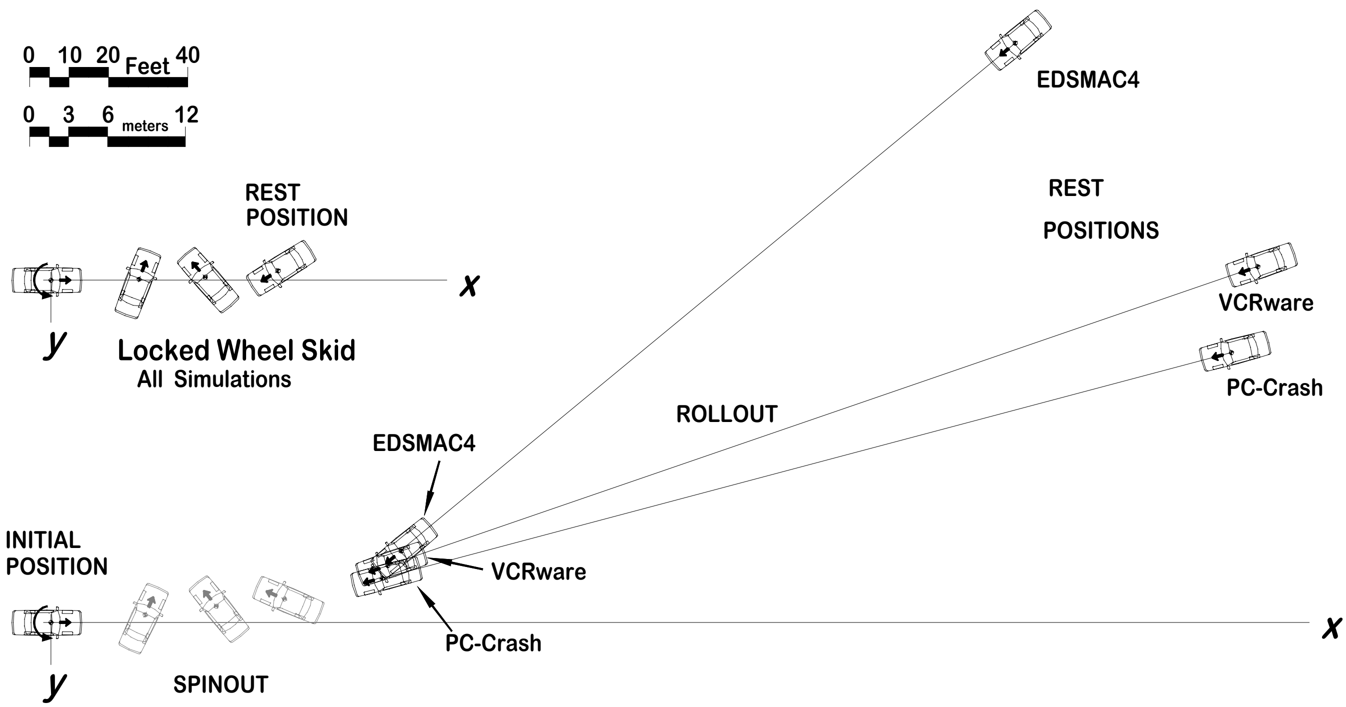


**Figure 15. Diagram of results of a locked wheel skid (Case A) and rolling resistance on the front wheels and powertrain drag on rear wheels (Case C), Crown Victoria.**

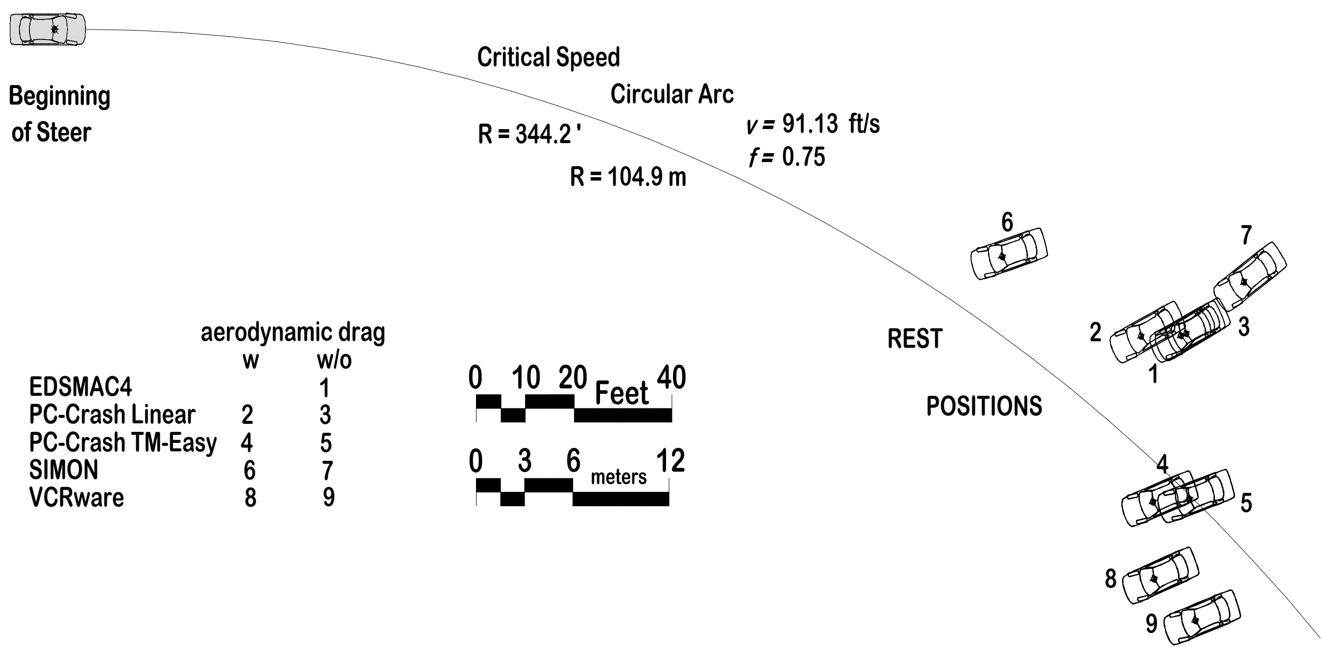


**Figure 16. Diagram of sudden steer maneuver simulation. "w" indicates aerodynamic drag is taken into account and "w/o" is with no aerodynamic drag. The circular arc is the path according to the critical speed formula.**

1991 Honda is listed as 195-60R15. It is important that these coefficients be reasonably accurate, yet tire parameter information from the open literature is sparse. In addition, tire properties for a given sized tire can vary from manufacturer to manufacturer. The tire parameters found and used here represent a reasonable set of values for this tire size but do not necessarily represent the exact values for the actual test vehicle. The values for this example were established in the following way.

Engineering Dynamics Corporation [HVE] lists a value for this tire as $C_\alpha$ = 231.7 lb/deg =13275 lb/rad for a vertical load of 1230 lb. Based on this, a value of $C_{\alpha f}$ = 13000 lb/rad is used for all simulations for the static normal force at the test vehicle front wheels, $W_f$ = 932 lb. Since tire side force coefficients vary with normal force and the static normal force for the rear of the test vehicle is approximately 660 lb, a value of $C_{\alpha r}$ must be estimated. An approximate formula can be developed (for small changes in normal force) from an equation in a paper on tires [Salaani], as

$$C_\alpha \approx kF_z \tag{68}$$

This gives

$$C_{\alpha r} \approx \frac{F_{zr}}{F_{zf}} C_{\alpha f} \tag{69}$$

giving a value of $C_{\alpha r}$ = 9200 lb/rad. This combination of values of $C_{\alpha f}$ and $C_{\alpha r}$ would place the 1991 Honda into a neutral steer condition (which is not the case). A second approach to estimate $C_{\alpha r}$ was taken using the front and rear Bundorf compliances [Milliken] for a passenger car. This gives

$$\frac{W_f C_{\alpha r}}{W_r C_{\alpha f}} = 1.1 \tag{70}$$

which, in turn gives $C_{\alpha r}$ = 10137 lb/rad. Based on these estimates, a value of $C_{\alpha r}$ = 10000 lb/rad was chosen for the static rear tire side force coefficients and used in all simulations. These values provide a static positive understeer gradient.

Figure 16 shows the rest positions and orientations from all of the simulations.

## DISCUSSION AND CONCLUSIONS

The primary purpose of this paper is to demonstrate that different tire models exist, to describe them in as much detail as possible and to indicate which simulation programs (used in accident reconstruction applications) use which tire models. Two example applications of these simulation programs and tire models are presented. The example applications were limited to a hypothetical postimpact motion of a Ford Crown Victoria and to a sudden steer maneuver of a Honda Accord. Results within the different simulations for each example are compared. Since the applications are limited to only two, the conclusions that can be drawn likewise are limited.

Alternative methods exist [Kiefer, et al., 2005, 2007] to estimate the combined effects of initial translational and rotational velocities on the trajectory of a vehicle to rest following impact that do not use tire force models. Such methods do not have the potential of simulating different tire properties and accident reconstruction conditions such as partial braking, powertrain drag, rolling wheel drag and/or the effects of an individually locked wheel or wheels. It is necessary to use a vehicle dynamic simulation program for modeling of such conditions. Despite the greater potential for accuracy, the uncertainty due to different tire models used in the simulation software cannot be overlooked. Differences do exist. All other things being equal, the more accurate the tire model, that is, the closer the tire model is to experimentally measured tire performance, the more accurate the simulation. Of course in accident reconstructions, accurate representation of the vehicles' physical parameters also is a factor that influences uncertainty.

In this paper, tire models and results of simulations for two cases that illustrate the wide ranges of $s$ and $\alpha$ typically found in accident reconstruction applications are presented. Differences in results can be attributed to model uncertainty. Differences between the simulations using the PC-Crash Linear Tire Model and the PC-Crash TM-Easy tire models are due only to the tire models. This is not true for comparisons between different simulation packages because other modeling differences exist (such as differences in suspension system models). Additional simulation comparisons need to be carried out before uncertainty due to tire models alone can discerned.

**Tire Force Models:** For combined braking and steering of an individual wheel, the PC-Crash Linear Tire Model is based on the process of first specifying the longitudinal (braking or accelerating) force, representing the lateral (steering) force with a bilinear curve and the use of the friction ellipse to compute the resultant tire force. For combined braking and steering of an individual wheel, the SMAC Tire Force Model (both EDSMAC4 and m-smac) is based on the process of first specifying the longitudinal (braking or accelerating) force, using the Fiala model for the lateral (steering) force and the use of the friction ellipse to compute the resultant tire force for combined steering and braking. The VCRware tire force model uses BNP equations with different parameters for the longitudinal and lateral forces and then uses the NCB equations for combined steering and braking. PC-crash allows the use of the Linear Tire Model or an alternative called the TM-Easy Model. The TM-Easy Model is based on a resultant wheel slip vector for combined steering and braking. The SIMON Tire Force Model is based on a modified HSRI Tire Model.

For the tire models covered in this paper two categories can be established. One category uses a specified level of braking (or acceleration) to establish the longitudinal tire force and the friction ellipse to calculate the combined longitudinal and lateral tire force components for combined steering and braking (PC-Crash Linear and SMAC Tire Models). The second category uses the direction of the wheel slip vector or slip velocity at the tire patch to determine the longitudinal and lateral tire force components for combined steering and braking (VCRware, PC-Crash TM-Easy and SIMON Tire models). Within each category, however, these models use different forms of equations to model the lateral tire forces (for no braking).

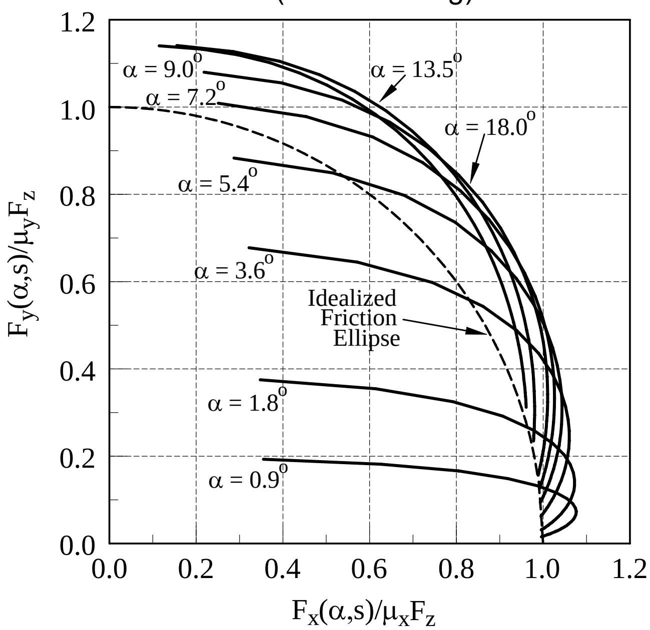


**Figure 17. Normalized BNP-BNC combined tire forces (solid curves) and the idealized friction ellipse (dashed curve) for $\mu_x = \mu_y$. The actual friction ellipse is the locus of points farthest from the origin that encompasses the tire combined forces.**

**Friction Ellipse:** It was shown that for relatively low slip angles, the use of the friction ellipse produces resultant forces equal in magnitude to a fully sliding tire. Some [Gäfvert & Svedenius] object to this feature. However, the use of the friction ellipse can actually *under-predict* combined tire forces. This is because the performance of models also depends on the functions used to represent the steering-alone and braking-alone curves, $F_x(s)$ and $F_y(\alpha)$. Figures 3 and 4 show that experimentally measured tire forces exceed the locked wheel skid force, $\mu F_z$, over some (early) regions of slip. Figure 17 is a plot of normalized BNP-NCB combined tire forces (which reflect measured characteristics) plotted on the friction ellipse coordinate system. The "friction ellipse" corresponding to the BNP-NCB tire forces is the locus of points of the curves for all values of $\alpha$ that lie a maximum radial distance from the origin (0,0). The friction ellipse for combined forces whose $F_x(s)$ and $F_y(\alpha)$ tire force curves do not exceed $\mu F_z$ is given by the dashed curve in Fig 17. As seen, the idealized friction ellipse can result in combined tire forces well below measured values.

**Simulation Comparisons:** More comparisons of the type presented and comparisons to experimental results are needed before any general conclusions concerning the influence of tire models on simulation accuracy can be drawn.

Different simulation models, with different tire models but the same initial conditions, have been found to produce different results for conditions of combined steering and braking. However, it cannot be concluded that the observed differences are due to the tire models alone from the present work. More research is necessary to determine the accuracy of the different tire models and different simulation software and for different categories of initial conditions and for different conditions of steering input. When used for purposes of accident reconstruction, differences in simulation results can be classified as model uncertainty. Such uncertainty must be recognized by accident reconstructionists.

## ACKNOWLEDGMENTS

The authors appreciate the cooperation of MEA Forensic Engineers and Scientists and for providing information and guidance with respect the PC-Crash Linear Tire model. The assistance of Terry Day of EngineeringDynamics Corporation is also gratefully appreciated. Finally, Prof. Dr. Georg Rill provided help and information with the formulation of the TM-Easy tire model.

## REFERENCES

ADAMS, http://www.mscsoftware.com/products/adams.cfm

Brach, Raymond and Matthew Brach, "Tire Models used in Accident Reconstruction Vehicle Motion Simulation", XVII Europäischen Vereinigung für Unfallforschung und Unfallanalyse (EVU) - Conference, Nice, France, 2008.

Brach, Raymond and Matthew Brach, "Tire

Forces: Modeling the Combined Braking and Steering Forces”, Paper 2000-01-0357, SAE, Warrendale, PA, 2000.

Brach, Raymond and Matthew Brach, *Vehicle Accident Analysis and Reconstruction Methods*, SAE, Warrendale, PA, 2005.

Car-Sim, http://www.carsim.com/

Cliff, W. E., J. M. Lawrence, B. E. Heinrichs and T. R. Fricker, “Yaw Testing of an Instrumented Vehicle with and Without Braking”, Paper 2004-01-1187, SAE, Warrendale, PA, 2004.

Daily, J., N. Shigemura and J. Daily, *Fundamentals of Traffic Crash Reconstruction, Volume 2 of the Traffic Crash Reconstruction Series* , IPTM, Jacksonville, FL, 2006.

EDC, Engineering Dynamics Corporation, *SIMON Simulation Model*, 5th Edition”, January 2006.

Fricke, L., (1) *Traffic Accident Reconstruction*, Northwestern University , Evanston, IL, 1990.

Fricke, L., (2) *Traffic Accident Reconstruction*, Volume 2, *Traffic Accident Investigation Manual*, Northwestern University , Evanston, IL, 1990.

Gäfvert, M. and J. Svedenius, “Construction of Novel Semi-Empirical Tire Models for Combined Braking and Cornering”, ISSN 0280-5316, Lund Institute of Technology, Sweden, 2003.

Guo, Konghui and Lei Ren, “A Unified Semi-Empirical Tire Model With Higher Accuracy and Less Parameters”, Paper 1999-01-0785, SAE International, Warrendale, PA, 1999.

Han, I. and S-U Park, “Inverse Analysis of Pre- and Post-Impact Dynamics for Vehicle Accident Reconstruction”, *Vehicle System Dynamics*, V 36, **6**, pp 413-433, 2001.

Hölscher, H., M. Tewes, N. Botkin, M. Lohndorf, K-H. Hoffman, and E. Quandt - Modeling of Pneumatic Tires by a Finite Element Model for the Development of a Tire Friction Remote Sensor, preprint submitted to *Computers and Structures*.

Hirschberg, W., G. Rill and H.Weinfurter, "User-Appropriate Tyre-Modelling for Vehicle Dynamics in Standard and Limit Situations," *Vehicle Systems Dynamics*, Vol. 38, No. 2, pp 103-125.

Hoerner, S. F., *Fluid-Dynamic Drag*, Hoerner Fluid Dynamics, Brick Town, NJ, 1965.

HVE, http://www.edccorp.com/products/hve.html

Keifer, O., B. Reckamp, T. Heilmann and P. Layson, “A Parametric Study of Frictional Resistance to Vehicular Rotation Resulting From a Motor Vehicle Impact”, Paper 2005-01-1203, SAE, Warrendale, PA, 2005.

Keifer, O., R. Conte and B. Reckamp, *Linear and Rotational Motion Analysis in Traffic Crash Reconstruction*, IPTM, Jacksonville, FL, 2007.

MacAdam, C., P. S. Fancher, T. H. Garrick, T. D. Gillespie, “A Computerized Model for Simulating the Braking and Steering Dynamics of Trucks, Tractor-Semitrailers, Doubles and Triples Combinations”, Highway Safety Research Institute., The University of Michigan (UM-HSRI-80-58).

Martinez, J. E. and R. J. Schleuter, “A Primer on the Reconstruction and Presentation of Rollover Accidents”, Paper 960647, SAE International, Warrendale, PA, 1996

McHenry, R., “Computer Program for Reconstruction of Highway Accidents”, Paper 730980, SAE Warrendale, PA, 1973

Milliken, W. F and D. L. Milliken, *Race Car Vehicle Dynamics*, SAE, Warrendale, PA, 1995

m-smac, http://www.mchenrysoftware.com/

Orlowski, K. R., E. A. Moffatt, R. T. Bundorf and M. P. Holcomb, “Reconstruction of Rollover Collisions”, Paper 890857, SAE International, Warrendale, PA, 1987.

Pacejka, Hans, *Tire and Vehicle Dynamics*, SAE, Warendale, PA, 2002

PC-Crash, http://www.meaforensic.com/technical/pc_crash.html

Pottinger, M. G., Pelz, W., and Falciola, G., "Effectiveness of the Slip Circle, "Combinator", Model for Combined Tire Cornering and Braking Forces When Applied to a Range of Tires", SAE Paper 982747, Warrendale, PA 15096.

Rill, G, *Vehicle Dynamics Lecture Notes*, University of Applied Sciences, Hochschule für Technik Wirtschaft Soziales, Germany, 2007.

Salaani, K., "Analytical Tire Forces and Moments Model with Validated Data", Paper 2007-01-0816, SAE International, Warrendale, PA, 2007.

Segal, J. *Highway Vehicle Object Simulation Model*, 4 Volumes (Users Manual, Programmers Manual, Engineering Manual-analysis, and Engineering Manual), 1422 pgs, Calspan Corporation, 1976.

Schuring, D. J., Pelz, W, Pottinger, M. G., "An Automated Implementation of the 'Magic Formula' Concept", SAE Paper 931909, Warrendale, PA 15096, 1993.

Tönük, E. and Y. S. Ünlüsoy, "Prediction of automobile tire cornering force characteristics by finite element modeling and analysis", *Computers and Structures*, 79 (2001), pp1219-1232.

VCRware, http://www.brachengineering.com/menu.swf

VDANL, http://www.systemstech.com/content/view/32/39/

## CONTACT

Raymond M. Brach
rbrach@nd.edu

R. Matthew Brach
matt_brach@brachengineering.com

**Table 1, Case A**

Locked Wheel Skid (SAE Coordinate System)

$\dot{x}_0 = 50\ ft/s\,(15.2\,m/s), \dot{y}_0 = 0, \dot{\theta}_0 = -150\,\deg/s$

**VCRware**

| | *x* | *y* | *θ* | *d* | *t* |
|---|---|---|---|---|---|
| Rest | 57.4 ft | 2.4 ft | -212° | 57.4 ft | 2.4 s |

**EDSMAC4**

| | *x* | *y* | *θ* | *d* | *t* |
|---|---|---|---|---|---|
| Rest | 57.4 ft | 2.3 ft | -215° | 57.4 ft | 2.3 s |

**PC-Crash** (Linear Tire Model)

| | *x* | *y* | *θ* | *d* | *t* |
|---|---|---|---|---|---|
| Rest | 57.0 ft | 2.4 ft | -211° | 57.1 ft | 2.3 s |

**Table 2, Case B**

Locked Right Front Wheel (SAE Coordinate System)

$\dot{x}_0 = 50\ ft/s\,(15.2\,m/s), \dot{y}_0 = 0, \dot{\theta}_0 = -150\,\deg/s$

**VCRware (*$E_{BNP}$* = 0.5)**

| | *x* | *y* | *θ* | *d* | *t* |
|---|---|---|---|---|---|
| Rest | 75.7 ft | -1.1 ft | -170° | 75.7 ft | 3.8 s |

**EDSMAC4**

| | *x* | *y* | *θ* | *d* | *t* |
|---|---|---|---|---|---|
| Rest | 81.3 ft | -1.4 ft | -182° | 82.1 ft | 4.1 s |

**PC-Crash** (Linear Tire Model)

| | *x* | *y* | *θ* | *d* | *t* |
|---|---|---|---|---|---|
| Rest | 77.6 ft | 0.3 ft | -173° | 77.6 ft | 4.0 s |

**Table 3, Case C**

Rolling Resistance and Power Train Drag (SAE Coordinate System)

$\dot{x}_0 = 50\,ft/s\,(15.2\,m/s), \dot{y}_0 = 0, \dot{\theta}_0 = -150\,\deg/s$

**VCRware ($E_{BNP}$ = 0.5)**

| | *x* | *y* | *θ* | *d* | *t* | |
|---|---|---|---|---|---|---|
| Rest | 305 ft | -91 ft | -199° | 318 ft | 19.4 s | |
| $\dot{\theta} = 0$: | 85 | -14 | -199° | 86 ft | 2.5 s | KE = 57373 J (42309 ft-lb) |

**EDSMAC4**

| | *x* | *y* | *θ* | *d* | *t* | |
|---|---|---|---|---|---|---|
| Rest | 242 ft | -149 ft | -220° | 284 ft | 18.5 s | |
| $\dot{\theta} = 0$: | 93 ft | -22 ft | -220° | 96 ft | 3.0 s | KE = 53181 J (39226 ft-lb) |

**PC-Crash** (Linear Tire Model)

| | *x* | *y* | *θ* | *d* | *t* | |
|---|---|---|---|---|---|---|
| Rest | 298 ft | -69 ft | -195° | 307 ft | 19.2 s | |
| $\dot{\theta} = 0$: | 84 ft | -11 ft | -195° | 85 ft | 2.3 s | KE = 59763 J (44079 ft-lb) |

**PC-Crash** (TM-Easy Tire Model)

| | *x* | *y* | *θ* | *d* | *t* | |
|---|---|---|---|---|---|---|
| Rest | 286 ft | -51 ft | -191° | 291 ft | 18.6 s | |
| $\dot{\theta} = 0$: | 75 ft | -10 ft | -191° | 76 ft | 2.1 s | KE = 56765 J (41868 ft-lb) |

## Appendix A. Three-dimensional plots of Tire Forces of Different Models

Three-dimensional surface plots of the tire forces (for combined braking and steering) from the different tire models are presented below.

Figures 18 through 25 are surface plots of the normalized tire forces for combined braking and steering for all of the models covered in this paper. Figures 18 and 19 are for the BNP-NCB tire model used by VCRware. Figure 20 shows the lateral force from PC-Crash Linear Tire Model for values for $0 \leq F_b/\mu F_z \leq 1$ and for $0 \leq \alpha \leq \pi/2$. Figure 21 shows the normalized lateral force from SMAC for $0 \leq T/\mu_x F_z \leq 1$ and for $0 \leq \alpha \leq \pi/2$. The longitudinal forces for PC-Crash Linear and SMAC models are not plotted since braking forces are specified directly as input to each program rather than being calculated as a function of wheel slip, *s*. Figures 22 and 23 are the longitudinal and lateral tire forces from the SIMON model, respectively. Finally, Fig 24 and 25 are plots of the TM-Easy tire forces.

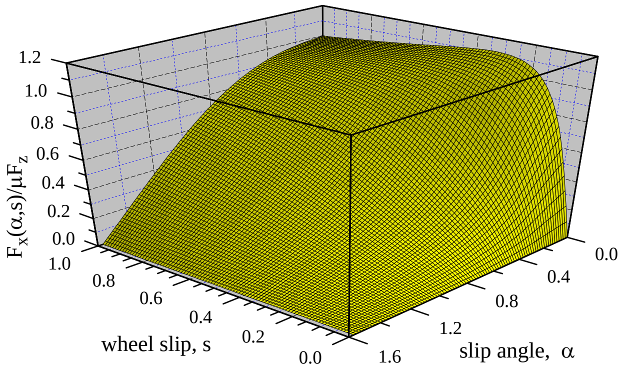


Figure 18. Normalized longitudinal tire force for combined braking and steering, VCRware

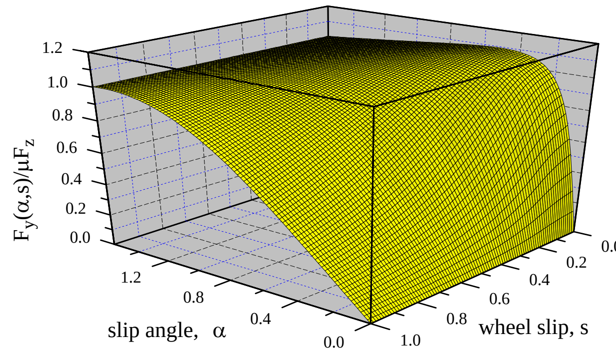


Figure 19. Normalized lateral force for combined braking and steering, VCRware.

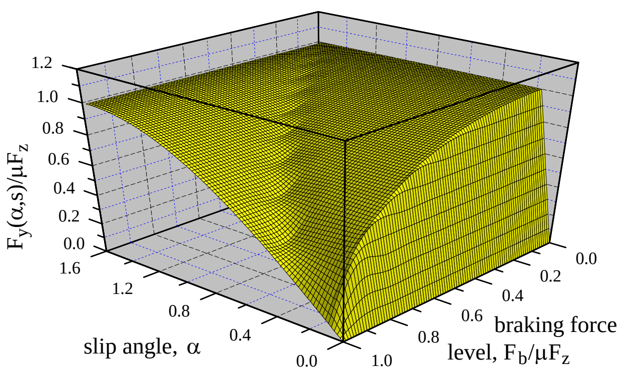


Figure 20. Normalized lateral tire force for combined braking and steering, PC-Crash linear Tire Model.

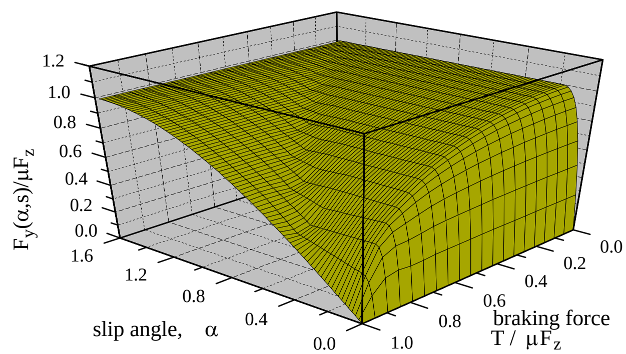


Figure 21. Normalized lateral tire force for combined braking and steering, SMAC

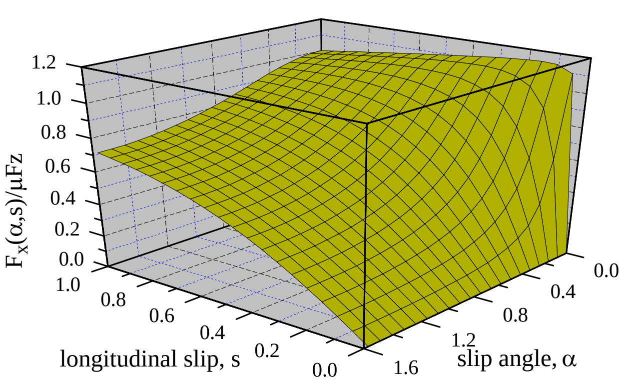


Figure 22. Normalized longitudinal tire force for combined braking and steering, SIMON.

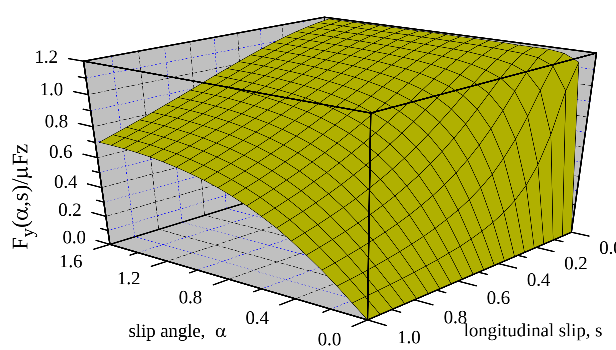


Figure 23. Normalized lateral tire force for combined braking and steering, SIMON.

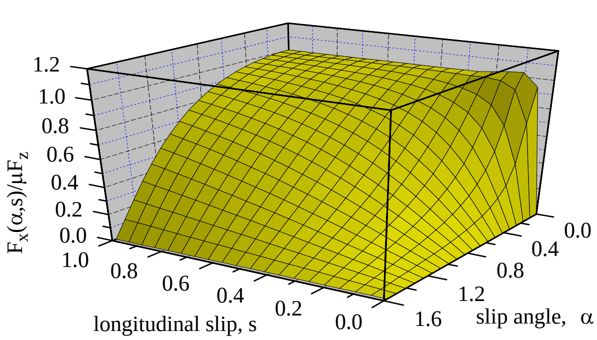


Figure 24. Normalized longitudinal tire force for combined braking and steering, TM-Easy.

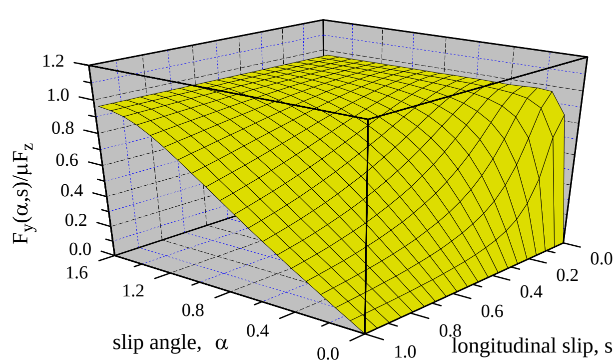


Figure 25. Normalized lateral tire force for combined braking and steering, TM-Easy.

## Appendix B: Specifications for Crown Victoria Spinout Example

Tire Coefficients

front: $C_{\alpha f}$ = 16000 lb/rad = 279.25 lb/deg = 71171.6 N/rad = 1242.18 N/deg

rear: $C_{\alpha r}$ = 14000 lb/rad = 244.35 lb/deg = 62275.1 N/rad = 1086.91 N/deg

Braking Coefficient

$C_s$ = 10000 lb = 44482.2 N

Rear Wheel Drag, 0.100 $\mu F_z$ Front Wheel Drag, 0.007 $\mu F_z$

Tire-road Frictional Drag Coefficient $f$ = 0.7

$F_z$: rear wheel, 892.5 lb = 3970.2 N = 404.9 kg

| | | | |
|---|---|---|---|
| Length | 212 in., 5.38 m | Wheelbase | 115 in., 2.92 m |
| Curb Weight | 4057 lb, 18.05 kN | Curb Weight Distribution | 56% /44% |
| Front Track | 63 in., 1.60 m | Rear Track | 66 in.1.68 m |
| Drive Wheels | Rear | Tire Size | P225/60R16 |
| Center of Gravity Ht | 22.37 in., 0.57 m | Yaw radius of gyration | $k$ = 4.86 ft = 1.48 m |

All other vehicle parameters, if any, are given by the software default parameters.

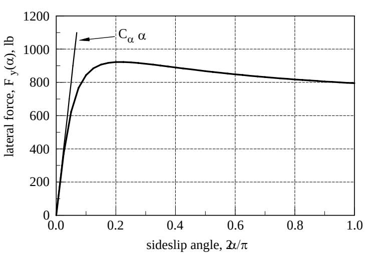


**Figure 26, *VCRware* lateral tire force, BNP: C = 1.5, E = 0.5**

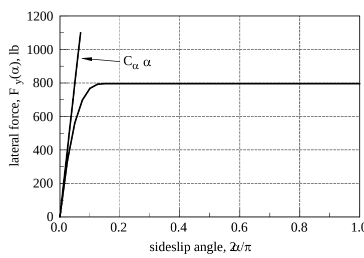


**Figure 27. *EDSMAC4* lateral tire force**

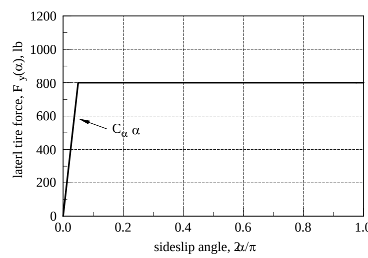


**Figure 28. *PC-Crash* lateral tire force**

## Appendix C: Specifications for Sudden Steer Maneuver

1991 Honda Accord EX

Vehicle weight, $W$ = 3186 lb, Distribution 61%/39%

Yaw Radius of Gyration, $k$ = 4.49 ft, 1.37 m

| | | | |
|---|---|---|---|
| Length | 185 in., 4.70 m | Wheelbase | 107 in., 2.72 m |
| Front Track | 58 in., 1.47 m | Rear Track | 58 in., 1.47 m |
| Tire Size | 195-60R15 | Center of Gravity Ht | 21.2 in, 0.54 m |

Tire Side Force Coefficients: $C_{\alpha F}$ = 13000 lb/rad, $C_{\alpha R}$ = 10000 lb/rad

Front Wheel Braking Force: 312.3 lb/wheel

Rear Wheel Braking Force: 122.9 lb/wheel

Initial Conditions: $x, y, \theta$ = 0,0,0, $\dot{x}, \dot{y}, \dot{\theta}$ = 91.134, 0, 0 ft/s

Front Wheel Steer Angle, $\delta$: linear rise from 0° to 9° in ½ sec, constant at 9°

Tire-road Frictional Drag Coefficient: 0.75

Aerodynamic Drag:

Coefficients (forward, lateral/side): $C_{dF}$ = 0.4, $C_{dL}$ = 0.8

Frontal, Lateral/side Areas: $A_F$ = 25 ft$^2$, $A_L$ = 60 ft$^2$

All other vehicle parameters, if any, are given by the software default parameters (see Appendix D).

# Appendix D: Lists of Simulation Programs input and Output

## D1: VCRware Input and Output, Crown Victoria Spinout Example:

vdynXL2008CrownVic.xls

1/29/2008

version 2.0

**VEHICLE DYNAMICAL SIMULATION**

| | Single Vehicle (or Tow Vehicle) | | | | Semitrailer | |
|---|---|---|---|---|---|---|
| | Weight, Wc, lb | Inertia, Jc, ft-lb-s^2 | | | Weight, Wt, lb | Inertia, Jt, ft-lb-s^2 |
| | 4057.0 | 2973.0 | | | 0.0 | 0.0 |
| | $L_1$ | $L_2$ | $L_3$ | $L_4$ | $L_5$ | $L_6$ |
| lengths, ft | 4.21 | 4.21 | 5.37 | 5.37 | 0.00 | 0.00 |
| | $W_1$ | $W_2$ | $W_3$ | $W_4$ | $W_5$ | $W_6$ |
| widths, ft | 2.63 | 2.63 | 2.75 | 2.75 | 0.00 | 0.00 |
| trailer/pin | | | $L_{CP}$ | $W_{CP}$ | $L_{TP}$ | $W_{TP}$ |
| dimensions, ft | | | 0.00 | 0.00 | 0.00 | 0.00 |
| center of gravity | $h_C$ | | | | $h_T$ | |
| heights, ft | 1.86 | | | | 0.00 | |
| tire lateral (steering) | $C_{\alpha 1}$ | $C_{\alpha 2}$ | $C_{\alpha 3}$ | $C_{\alpha 4}$ | $C_{\alpha 5}$ | $C_{\alpha 6}$ |
| coefficients, lb/rad | 16000.0 | 16000.0 | 14000.0 | 14000.0 | 0.0 | 0.0 |
| tire forward (braking) | $C_{s1}$ | $C_{s2}$ | $C_{s3}$ | $C_{s4}$ | $C_{s5}$ | $C_{s6}$ |
| coefficients, lb | 10000.0 | 10000.0 | 10000.0 | 10000.0 | 0.0 | 0.0 |
| wheel brake slip | $s_1$ | $s_2$ | $s_3$ | $s_4$ | $s_5$ | $s_6$ |
| values, 0 < s < 1 | 0.0010 | 0.0010 | 0.0109 | 0.0109 | 0.000 | 0.000 |
| wheel acceleration | | vehicle uniform accel, g's | | 0.00 | | |
| traction coefficients | 0 | 0 | 0 | 0 | 0 | 0 |
| aero drag coeffs and | $C_DA_{XC}$ | $C_DA_{YC}$ | $W_X$ | $W_Y$ | $C_DA_{XT}$ | $C_DA_{YT}$ |
| wind speeds, W, ft/s | 0.00 | 0.00 | 0.00 | 0.00 | 0.00 | 0.00 |
| | | | | $L_C$ | | $L_T$ |
| | | | | 0.00 | | 0.00 |
| | Xc, ft | Xc - dot, ft/s | Yc, ft | Yc - dot, ft/s | | |
| initial conditions | 0.00 | 50.00 | 0.00 | 0.00 | | |
| | $\theta_C$, deg | $\theta_C$ - dot, °/s | | | $\theta_T$ | $\theta_T$ - dot |
| initial conditions | 0.00 | -150.00 | | | 0.00 | 0.00 |
| steer angle, δ, deg | 0.000 | | | | | |
| g, ft/s^2 | 32.17 | | | | | |

2006 FORD
CROWN VICTORIA
P22560R16
0.7% front/10%rear

| | | | friction coefficients | |
|---|---|---|---|---|
| | $R_W$, road | | road | shoulder |
| roadway | width, ft | | $f_R$ | $f_B$ |
| parameters | 24.0 | | 0.70 | 0.70 |
| | integration | print | steering | number of |
| program | interval, s | interval | mode, KM | wheels |
| run | 0.0050 | 100 | 1 | 4 |
| parameters | final time, s | | | 1 |
| | 50.00 | | KM | mode |
| | | | -1 | tabular steer (S5:T25) |
| | lane change | | 0 | all wheels locked |
| | duration | 4.00 | 1 | lane change |

no trailer US

MEQ (0/1)

Run vdynXL

Unit Conversion

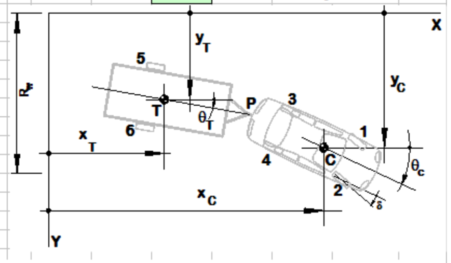


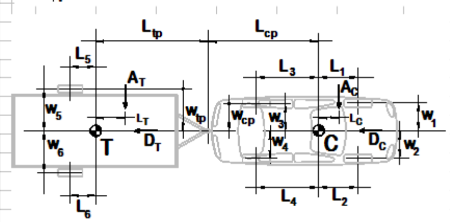


Brach Engineering

VCRware™

Vehicle Crash Reconstruction Software

www.brachengineering.com

| | | Front Wheel Steer Solution, KM = 1 | | | | | | | |
|---|---|---|---|---|---|---|---|---|---|
| time, t | $X_c$ | $X_c$ - Vel | $Y_c$ | $Y_c$ - Vel | $\theta_c$ | $\theta_c$ - Vel | $\theta_T$ | $\theta_T$ - Vel | δ |
| sec | ft | ft/s | ft | ft/s | deg | deg/s | deg | deg/s | deg |
| 0.000 | 0.00 | 50.00 | 0.00 | 0.00 | 0.00 | -150.00 | | | 0.000 |
| 0.500 | 23.97 | 43.88 | -1.74 | -7.63 | -63.47 | -124.98 | | | 0.000 |
| 1.000 | 43.08 | 32.87 | -5.85 | -6.74 | -126.27 | -125.98 | | | 0.000 |
| 1.500 | 58.00 | 28.73 | -7.28 | -1.23 | -184.06 | -69.90 | | | 0.000 |
| 2.000 | 71.88 | 26.42 | -9.29 | -7.48 | -198.43 | -7.33 | | | 0.000 |
| 2.500 | 84.71 | 25.17 | -13.56 | -8.79 | -199.28 | -0.08 | | | 0.000 |
| 3.000 | 97.12 | 24.44 | -17.90 | -8.56 | -199.29 | 0.00 | | | 0.000 |
| 3.500 | 109.16 | 23.72 | -22.11 | -8.30 | -199.29 | 0.00 | | | 0.000 |
| 4.000 | 120.84 | 23.00 | -26.20 | -8.05 | -199.29 | 0.00 | | | 0.000 |
| 4.500 | 132.16 | 22.29 | -30.16 | -7.80 | -199.29 | 0.00 | | | 0.000 |
| 5.000 | 143.12 | 21.57 | -34.00 | -7.55 | -199.29 | 0.00 | | | 0.000 |
| 5.500 | 153.73 | 20.85 | -37.71 | -7.30 | -199.29 | 0.00 | | | 0.000 |
| 6.000 | 163.97 | 20.13 | -41.30 | -7.04 | -199.29 | 0.00 | | | 0.000 |
| 6.500 | 173.86 | 19.41 | -44.75 | -6.79 | -199.29 | 0.00 | | | 0.000 |
| 7.000 | 183.38 | 18.69 | -48.09 | -6.54 | -199.29 | 0.00 | | | 0.000 |
| 7.500 | 192.55 | 17.97 | -51.30 | -6.29 | -199.29 | 0.00 | | | 0.000 |
| 8.000 | 201.35 | 17.25 | -54.38 | -6.04 | -199.29 | 0.00 | | | 0.000 |
| 8.500 | 209.80 | 16.53 | -57.33 | -5.79 | -199.29 | 0.00 | | | 0.000 |
| 9.000 | 217.88 | 15.81 | -60.16 | -5.53 | -199.29 | 0.00 | | | 0.000 |
| 9.500 | 225.61 | 15.09 | -62.87 | -5.28 | -199.29 | 0.00 | | | 0.000 |
| 10.000 | 232.97 | 14.37 | -65.45 | -5.03 | -199.29 | 0.00 | | | 0.000 |
| 10.500 | 239.98 | 13.65 | -67.90 | -4.78 | -199.29 | 0.00 | | | 0.000 |
| 11.000 | 246.63 | 12.93 | -70.22 | -4.53 | -199.29 | 0.00 | | | 0.000 |
| 11.500 | 252.91 | 12.21 | -72.42 | -4.27 | -199.29 | 0.00 | | | 0.000 |
| 11.999 | 258.84 | 11.49 | -74.50 | -4.02 | -199.29 | 0.00 | | | 0.000 |
| 12.499 | 264.41 | 10.77 | -76.45 | -3.77 | -199.29 | 0.00 | | | 0.000 |
| 12.999 | 269.62 | 10.05 | -78.27 | -3.52 | -199.29 | 0.00 | | | 0.000 |
| 13.499 | 274.46 | 9.34 | -79.97 | -3.27 | -199.29 | 0.00 | | | 0.000 |
| 13.999 | 278.95 | 8.62 | -81.54 | -3.02 | -199.29 | 0.00 | | | 0.000 |
| 14.499 | 283.08 | 7.90 | -82.98 | -2.76 | -199.29 | 0.00 | | | 0.000 |
| 14.999 | 286.85 | 7.18 | -84.30 | -2.51 | -199.29 | 0.00 | | | 0.000 |
| 15.499 | 290.26 | 6.46 | -85.49 | -2.26 | -199.29 | 0.00 | | | 0.000 |
| 15.999 | 293.31 | 5.74 | -86.56 | -2.01 | -199.29 | 0.00 | | | 0.000 |
| 16.499 | 296.00 | 5.02 | -87.50 | -1.76 | -199.29 | 0.00 | | | 0.000 |
| 16.999 | 298.33 | 4.30 | -88.32 | -1.50 | -199.29 | 0.00 | | | 0.000 |
| 17.499 | 300.30 | 3.58 | -89.01 | -1.25 | -199.29 | 0.00 | | | 0.000 |
| 17.999 | 301.91 | 2.86 | -89.57 | -1.00 | -199.29 | 0.00 | | | 0.000 |
| 18.499 | 303.16 | 2.14 | -90.01 | -0.75 | -199.29 | 0.00 | | | 0.000 |
| 18.999 | 304.05 | 1.42 | -90.32 | -0.50 | -199.29 | 0.00 | | | 0.000 |
| 19.330 | 304.44 | 0.95 | -90.46 | -0.33 | -199.29 | 0.00 | | | 0.000 |

| | | | | | | | | | | | | |
|---|---|---|---|---|---|---|---|---|---|---|---|---|
| | | **Front Wheel Steer Solution, KM = 1** | | | | | | | | | | |
| | | | | | | | | | | | | |
| **Static Normal Forces, lb** | | | | | | | | | | | | |
| **1137.1** | **1137.1** | **891.4** | **891.4** | **0.0** | **0.0** | **Full Equil** | | f (ROAD) | 0.70 | | | |
| 1137.1 | 1137.1 | 891.4 | 891.4 | 0.0 | 0.0 | **$M_{EQ} = 0$** | | f (OFF ROAD) | 0.70 | | | |
| | | | | | | | | | | | | |
| | **LF** | | **RF** | | **LR** | | **RR** | | **TL** | | **TR** | |
| | **wheel 1** | friction | **wheel 2** | friction | **wheel 3** | friction | **wheel 4** | friction | **wheel 5** | friction | **wheel 6** | friction |
| time, s | total force | limit, lb | total force | limit, lb | total force | limit, lb | total force | limit, lb | total force | limit, lb | total force | limit, lb |
| 0.000 | 0.0% | 795.9 | 0.0% | 795.9 | 0.0% | 624.0 | 0.0% | 624.0 | | | | |
| 0.500 | 106.7% | 425.7 | 110.1% | 1165.6 | 103.1% | 254.4 | 106.2% | 994.3 | | | | |
| 1.000 | 108.2% | 439.1 | 103.4% | 1150.0 | 103.6% | 269.9 | 101.5% | 980.9 | | | | |
| 1.500 | 110.8% | 830.1 | 117.0% | 748.6 | 112.5% | 671.3 | 118.9% | 589.8 | | | | |
| 2.000 | 60.5% | 958.3 | 83.1% | 608.5 | 24.3% | 811.4 | 40.4% | 461.6 | | | | |
| 2.500 | 1.6% | 786.1 | 1.6% | 779.6 | 13.8% | 640.3 | 13.9% | 633.8 | | | | |
| 3.000 | 1.0% | 782.9 | 1.0% | 782.9 | 13.8% | 637.1 | 13.8% | 637.0 | | | | |
| 3.500 | 1.0% | 782.9 | 1.0% | 782.9 | 13.8% | 637.1 | 13.8% | 637.1 | | | | |
| 4.000 | 1.0% | 782.9 | 1.0% | 782.9 | 13.8% | 637.1 | 13.8% | 637.1 | | | | |
| 4.500 | 1.0% | 782.9 | 1.0% | 782.9 | 13.8% | 637.1 | 13.8% | 637.1 | | | | |
| 5.000 | 1.0% | 782.9 | 1.0% | 782.9 | 13.8% | 637.1 | 13.8% | 637.1 | | | | |
| 5.500 | 1.0% | 782.9 | 1.0% | 782.9 | 13.8% | 637.1 | 13.8% | 637.1 | | | | |
| 6.000 | 1.0% | 782.9 | 1.0% | 782.9 | 13.8% | 637.1 | 13.8% | 637.1 | | | | |
| 6.500 | 1.0% | 782.9 | 1.0% | 782.9 | 13.8% | 637.1 | 13.8% | 637.1 | | | | |
| 7.000 | 1.0% | 782.9 | 1.0% | 782.9 | 13.8% | 637.1 | 13.8% | 637.1 | | | | |
| 7.500 | 1.0% | 782.9 | 1.0% | 782.9 | 13.8% | 637.1 | 13.8% | 637.1 | | | | |
| 8.000 | 1.0% | 782.9 | 1.0% | 782.9 | 13.8% | 637.1 | 13.8% | 637.1 | | | | |
| 8.500 | 1.0% | 782.9 | 1.0% | 782.9 | 13.8% | 637.1 | 13.8% | 637.1 | | | | |
| 9.000 | 1.0% | 782.9 | 1.0% | 782.9 | 13.8% | 637.1 | 13.8% | 637.1 | | | | |
| 9.500 | 1.0% | 782.9 | 1.0% | 782.9 | 13.8% | 637.1 | 13.8% | 637.1 | | | | |
| 10.000 | 1.0% | 782.9 | 1.0% | 782.9 | 13.8% | 637.1 | 13.8% | 637.1 | | | | |
| 10.500 | 1.0% | 782.9 | 1.0% | 782.9 | 13.8% | 637.1 | 13.8% | 637.1 | | | | |
| 11.000 | 1.0% | 782.9 | 1.0% | 782.9 | 13.8% | 637.1 | 13.8% | 637.1 | | | | |
| 11.500 | 1.0% | 782.9 | 1.0% | 782.9 | 13.8% | 637.1 | 13.8% | 637.1 | | | | |
| 11.999 | 1.0% | 782.9 | 1.0% | 782.9 | 13.8% | 637.1 | 13.8% | 637.1 | | | | |
| 12.499 | 1.0% | 782.9 | 1.0% | 782.9 | 13.8% | 637.1 | 13.8% | 637.1 | | | | |
| 12.999 | 1.0% | 782.9 | 1.0% | 782.9 | 13.8% | 637.1 | 13.8% | 637.1 | | | | |
| 13.499 | 1.0% | 782.9 | 1.0% | 782.9 | 13.8% | 637.1 | 13.8% | 637.1 | | | | |
| 13.999 | 1.0% | 782.9 | 1.0% | 782.9 | 13.8% | 637.1 | 13.8% | 637.1 | | | | |
| 14.499 | 1.0% | 782.9 | 1.0% | 782.9 | 13.8% | 637.1 | 13.8% | 637.1 | | | | |
| 14.999 | 1.0% | 782.9 | 1.0% | 782.9 | 13.8% | 637.1 | 13.8% | 637.1 | | | | |
| 15.499 | 1.0% | 782.9 | 1.0% | 782.9 | 13.8% | 637.1 | 13.8% | 637.1 | | | | |
| 15.999 | 1.0% | 782.9 | 1.0% | 782.9 | 13.8% | 637.1 | 13.8% | 637.1 | | | | |
| 16.499 | 1.0% | 782.9 | 1.0% | 782.9 | 13.8% | 637.1 | 13.8% | 637.1 | | | | |
| 16.999 | 1.0% | 782.9 | 1.0% | 782.9 | 13.8% | 637.1 | 13.8% | 637.1 | | | | |
| 17.499 | 1.0% | 782.9 | 1.0% | 782.9 | 13.8% | 637.1 | 13.8% | 637.1 | | | | |
| 17.999 | 1.0% | 782.9 | 1.0% | 782.9 | 13.8% | 637.1 | 13.8% | 637.1 | | | | |
| 18.499 | 1.0% | 782.9 | 1.0% | 782.9 | 13.8% | 637.1 | 13.8% | 637.1 | | | | |
| 18.999 | 1.0% | 782.9 | 1.0% | 782.9 | 13.8% | 637.1 | 13.8% | 637.1 | | | | |
| 19.330 | 1.0% | 782.9 | 1.0% | 782.9 | 13.8% | 637.1 | 13.8% | 637.1 | | | | |

**D2: PC-Crash Linear Tire Model, w/ aero drag, Vehicle: 1991 Honda-Accord**

**START VALUES**

| | |
|---|---|
| Velocity magnitude (v) [ft/s] : | 91.13 |
| Heading angle [deg] : | 0.00 |
| Velocity direction (ß) [deg] : | 0.00 |
| Yaw velocity [Deg/s] : | 0.00 |
| Center of gravity x [ft] : | 0.00 |
| Center of gravity y [ft] : | 0.00 |
| Center of gravity z [ft] : | 1.76 |
| Velocity vertical [ft/s] : | -0.00 |
| Roll angle [deg] : | -0.00 |
| Pitch angle [deg] : | 0.00 |
| Roll velocity [Deg/s] : | 0.00 |
| Pitch velocity [Deg/s] : | 0.00 |

**END VALUES**

| | |
|---|---|
| Velocity magnitude (v) [ft/s] : | 0.53 |
| Heading angle [deg] : | -153.51 |
| Velocity direction (ß) [deg] : | 7.99 |
| Yaw velocity [Deg/s] : | 0.54 |
| Center of gravity x [ft] : | 222.15 |
| Center of gravity y [ft] : | -55.43 |
| Center of gravity z [ft] : | 1.77 |
| Velocity vertical [ft/s] : | -0.00 |
| Roll angle [deg] : | -0.06 |
| Pitch angle [deg] : | -0.79 |
| Roll velocity [Deg/s] : | -3.84 |
| Pitch velocity [Deg/s] : | 0.11 |

**SEQUENCES**

1 1991 HON :

**START VALUES**

| | |
|---|---|
| Velocity [ft/s] : | 91.13 |
| Friction coefficient : | 0.75 |

**BRAKE**

| | | |
|---|---|---|
| maximum stopping distance [ft] : | | 300.00 |
| Brake force [%] | | |
| Axle 1, left : | 33.50 | |
| Axle 1, right : | 33.50 | |
| Axle 2, left : | 18.60 | |
| Axle 2, right : | 18.60 | |
| mean brake acceleration [g] : | | -0.27 |

**STEERING**

| | |
|---|---|
| Steering time [s] : | 0.50 |
| New steering angle [deg] | |
| Axle 1 : | -9.00 |
| Axle 2 : | 0.00 |
| Turning circle [ft] : | -114.00 |

**INPUT VALUES**

| | |
|---|---|
| Vehicle : | 1991 Honda-Accord |
| Length [in] : | 160.80 |
| Width [in] : | 67.00 |
| Height [in] : | 53.73 |
| Number of axles : | 2.00 |
| Wheelbase [in] : | 107.00 |
| Front overhang [in] : | 34.00 |
| Front track width [in] : | 58.00 |
| Rear track width [in] : | 58.00 |
| Mass (empty) [lb] : | 3186.00 |
| Mass of front occupants [lb] : | 0.00 |
| Mass of rear occupants [lb] : | 0.00 |
| Mass of cargo in trunk [lb] : | 0.00 |
| Mass of roof cargo [lb] : | 0.00 |
| Distance C.G. - front axle [in] : | 44.40 |
| C.G. height above ground [in] : | 21.12 |
| Roll moment of inertia [lbfts^2] : | 450.30 |
| Pitch moment of inertia [lbfts^2] : | 1500.90 |
| Yaw moment of inertia [lbfts^2] : | 2000.00 |
| Stiffness, axle 1, left [lb/in] : | 121.93 |
| Stiffness, axle 1, right [lb/in] : | 121.93 |
| Stiffness, axle 2, left [lb/in] : | 121.93 |
| Stiffness, axle 2, right [lb/in] : | 121.93 |
| Damping, axle 1, left [lb-s/ft] : | 164.60 |
| Damping, axle 1, right [lb-s/ft] : | 164.60 |
| Damping, axle 2, left [lb-s/ft] : | 164.60 |
| Damping, axle 2, right [lb-s/ft] : | 164.60 |
| Linear Tire Model: | |
| Max slip angle,axle 1, left [deg]: | 4.11 |
| Max slip angle,axle 1, right [deg]: | 4.11 |
| Max slip angle,axle 2, left [deg]: | 3.44 |
| Max slip angle,axle 2, right [deg]: | 3.44 |
| $C_{\alpha f}$ = 13,000 lb/rad | |
| $C_{\alpha r}$ = 10,000 lb/rad | |
| ABS : | No |

**SECTIONS**

1 1991 HONDA:

| | Time [s], | Dist. [ft], | Vel. [ft/s] |
|---|---|---|---|
| Start (t=0s) | -0.00 | 0.00 | 91.1 |
| Brake | 5.15 | 232.60 | 0.4 |

## D3: SIMON, w/ aero drag, Vehicle: 1991 Honda-Accord

----- ACCIDENT HISTORY -----

| | time (sec) | X (m) | Y (m) | Heading (deg) | Vtot (km/h) | U (km/h) | V (km/h) | Yaw Vel (deg/sec) |
|---|---|---|---|---|---|---|---|---|
| -Start of Simulation- | | | | | | | | |
| Honda Accord 4-Dr - S | 0.0000 | 0.0 | -30.5 | 0.0 | 113.0 | 113.0 | 0.0 | 0.0 |
| --- At Final/Rest --- | | | | | | | | |
| Honda Accord 4-Dr - S | 6.1157 | 90.0 | -12.9 | 160.9 | 0.0 | 0.0 | 0.0 | 0.0 |

-------------- DRIVER CONTROLS -----------------

Driver Controls for: Honda Accord 4-Dr - SIMON

DRIVER CONTROL TABLES (OPEN-LOOP)

Steer Table:

| Time (sec) | Axle 1 Right (deg) | Axle 1 Left (deg) |
|---|---|---|
| 0.0000 | 0.00 | 0.00 |
| 1.0000 | 0.00 | 0.00 |
| 1.5000 | 9.00 | 9.00 |

Brake Table:

| Time (sec) | Pedal Force (N) |
|---|---|
| 0.0000 | 0.00 |
| 1.0000 | 0.00 |
| 1.1000 | 18.00 |

Throttle Table:

| Time (sec) | Throttle Position (%/100) |
|---|---|
| 0.0000 | 0.00 |

Transmission Shift Table: (No Transmission Table)

Differential Shift Table: (No Differential Table)

GENERAL ENVIRONMENT DATA

| | |
|---|---|
| Ambient Temperature (Celsius): | 20.00 |
| Ambient Pressure (kPa): | 101.32 |
| Air Density (kg/m^3): | 1.2045 |
| Wind Speed (km/h): | 0.00 |
| Wind Direction (deg): | 0.00 |
| Gravity Constant (m/sec^2): | 9.81 |

3-D ENVIRONMENT TERRAIN DATA

| | |
|---|---|
| 3-D Geometry Filename: | (Unknown) |
| Number of Polygons: | 10 |
| GetSurfaceInfo: | From Previous Polygon |
| Minimum Terrain Elevation (m): | 0.00 |
| Maximum Terrain Elevation (m): | 0.00 |

## GENERAL PROGRAM INFORMATION

| | |
|---|---|
| SIMON Version No: | 3.20 |

**Simulation Controls ---**

| | |
|---|---|
| Integration Method: | Fixed Runge-Kutta |
| Maximum Simulation Time (sec): | 10.0000 |
| Integration Timestep (sec): | 0.0010 |
| Output Interval (sec): | 0.0010 |
| Linear Term Vel (km/h): | 0.17 |
| Angular Term Vel (deg/sec): | 5.00 |

**Calculation Options ---**

| | |
|---|---|
| GetSurfaceInfo: | From Previous Polygon |
| Tire Model Method: | Semi-empirical |
| Steer Degree Of Freedom: | Off |
| Articulation Option: | On |
| DyMESH Option: | Off |

## VEHICLE DATA

**General Information ---**

| | |
|---|---|
| Vehicle Name: | Honda Accord 4-Dr - SIMON |
| Vehicle Type: | Passenger Car |
| Vehicle Make: | Honda |
| Vehicle Model: | Accord |
| Vehicle Year: | 1990-1993 |
| Vehicle Body Style: | 4-Door |
| Version No: | V 5.20 (RCS $Revision: 2.3 |
| Number of Axles: | 2 |
| Driver Location: | Left Side |
| Engine Location: | Front Engine |
| Drive Axle(s): | Axle 1 |

**Sprung Mass Dimensional Data ---**

| | |
|---|---|
| Overall Length (cm): | 467.36 |
| Overall Width (cm): | 172.47 |
| Overall Height (cm): | 137.55 |
| Ground Clearance (cm): | 23.25 |
| Wheelbase (cm): | 272.00 |
| CG to Front Axle (cm): | 106.00 |
| CG to Back Axle (cm): | -166.00 |
| CG Height (cm): | 54.00 |
| Front Overhang (cm): | 89.23 |
| Rear Overhang (cm): | 106.13 |

**Sprung Mass Inertial Data ---**

| | |
|---|---|
| Total Weight (N): | 14172.03 |
| Sprung Weight (N): | 13440.52 |
| Sprung Mass (kg): | 1369.45 |
| Sprg Mass Rot Inertia (kg-m^2) - Roll: | 352.96 |
| Pitch: | 2574.11 |
| Yaw: | 2527.54 |
| XZ Product: | 0.00 |

**Sprung Mass Aerodynamic Parameters ---**

| | |
|---|---|
| Surface Name: | Left |
| Drag Coefficient: | 0.8000 |
| Proj. Surface Area (cm^2): | 55741.82 |
| Center of Pressure (cm) - x: | -23.11 |
| y: | -83.82 |
| z: | 0.00 |

**Brake System Data ---**

| | |
|---|---|
| Brake Pedal Ratio (kPa/N): | 27.22 |
| ABS System: | None Installed |

**Steering System Parameters ---**

| | |
|---|---|
| First Axle: | Steerable |
| Steering Gear Ratio (deg/deg): | 16.62 |

| | Right Side | Left Side |
|---|---|---|
| Caster (deg): | 3.00 | 3.00 |
| Inclination Angle (deg): | 6.83 | 6.83 |
| Steering Offset (cm): | 0.43 | 0.43 |
| Stub Axle Length (cm): | 4.35 | 4.35 |
| Initial Steer Axis Coord (cm) - x: | 106.00 | 106.00 |
| y: | 71.29 | -67.01 |

| | | | | | |
|---|---|---|---|---|---|
| 10.16 | 0.00 | 0.00 | 10.16 | 0.00 | 0.00 |

Tire Information, First Axle ---

| | Right Side | Left Side |
|---|---|---|
| Tire Name: | Generic | Generic |
| Tire Manufacturer: | Generic | Generic |
| Tire Model: | Generic | Generic |
| Tire Size: | P195/60R15 | P195/60R15 |
| Version No: | es\db\E | es\db\E |
| Unloaded Radius (cm): | 30.75 | 30.75 |
| Init. Radial Stiffness (N/cm/tire): | 2637.99 | 2637.99 |
| 2nd Radial Stiffness (N/cm/tire): | 26379.88 | 26379.88 |
| Defl. @ 2nd Stiffness (cm): | 9.36 | 9.36 |
| Max Deflection (cm): | 11.70 | 11.70 |
| Rebound Energy Ratio (%/100): | 1.00 | 1.00 |
| Spin Inertia (Tire+Whl+Brk, kg-m^2/tire) | 0.89 | 0.89 |
| Steer Inertia (Tire+Whl+Brk, kg-m^2/tire | 0.44 | 0.44 |
| Weight (Tire+Whl+Brk, N/tire): | 182.88 | 182.88 |
| Roll Resistance Const: | 0.01 | 0.01 |
| Roll Resististance Linear Coef (sec/m): | 0.00 | 0.00 |
| Min Fz For Skidmark (N): | 1370.05 | 1370.05 |
| Pneumatic Trail (cm): | -2.19 | -2.19 |
| Lateral Stiffness (N/cm): | 2637.99 | 2637.99 |

| Cornering Stiffness (N/deg/tire): | Right Side | | | Left Side | | |
|---|---|---|---|---|---|---|
| Loads (N): | 2701.4 | 5471.8 | 8210.1 | 2701.4 | 5471.8 | 8210.1 |
| Speeds (m/sec): | 13.4 | | | 13.4 | | |
| Load No.: | 1 | 2 | 3 | 1 | 2 | 3 |
| Speed No. 1: | 1005.3 | 1005.3 | 1005.3 | 1005.3 | 1005.3 | 1005.3 |

| Camber Stiffness (N/deg/tire): | Right Side | | | Left Side | | |
|---|---|---|---|---|---|---|
| Loads (N): | 2727.6 | 5496.7 | 8259.5 | 2727.6 | 5496.7 | 8259.5 |
| Speeds (m/sec): | 13.4 | | | 13.4 | | |
| Load No.: | 1 | 2 | 3 | 1 | 2 | 3 |
| Speed No. 1: | 22.3 | 55.7 | 85.5 | 22.3 | 55.7 | 85.5 |

| Tire Friction Table: | Right Side | | | Left Side | | |
|---|---|---|---|---|---|---|
| Loads (N): | 2740.1 | 5466.9 | 8193.6 | 2740.1 | 5466.9 | 8193.6 |
| Speeds (m/sec): | 13.4 | | | 13.4 | | |
| Speed No. 1, Load No.: | 1 | 2 | 3 | 1 | 2 | 3 |
| Peak Mu: | 1.0500 | 1.0500 | 1.0500 | 1.0500 | 1.0500 | 1.0500 |
| Slide Mu: | 0.7500 | 0.7500 | 0.7500 | 0.7500 | 0.7500 | 0.7500 |
| Slip @ Peak Mu (%/100): | 0.2440 | 0.1680 | 0.1460 | 0.2440 | 0.1680 | 0.1460 |
| Long. Stiffness (N/slip): | 58574.2 | 103123.1 | 184828.1 | 58574.2 | 103123.1 | 184828.1 |

Brake Information, First Axle ---

| | Right Side | Left Side |
|---|---|---|
| Brake Assembly Type: | Generic Brake | Generic Brake |
| Brake Time Lag (sec): | 0.0000 | 0.0000 |
| Brake Time Rise (sec): | 0.0000 | 0.0000 |
| Pushout Pressure (kPa): | 0.00 | 0.00 |
| Nominal Brake Torque Ratio (N-m/kPa): | 0.38 | 0.38 |

Wheel Location Information, Second Axle ---

| | Right Side | Left Side |
|---|---|---|
| Initial Wheel Coordinates (cm) - x: | -166.00 | -166.00 |
| y: | 75.64 | -71.36 |

| | Right Side | Left Side |
|---|---|---|
| z: | 23.25 | 23.25 |

Suspension Information, Second Axle ---

Suspension Type: Independent

Auxiliary Roll Stiffness (N-m/deg): 0.00

| | Right Side | Left Side |
|---|---|---|
| Spring Rate (N/cm): | 185.11 | 185.11 |
| Viscous Damping (N-sec/m): | 1208.38 | 1208.38 |
| Coulomb Friction (N): | 222.41 | 222.41 |
| Friction Null Band (cm/sec): | 12.70 | 12.70 |
| Deflection to Jounce Stop (cm): | -10.16 | -10.16 |
| Stop Linear Rate (N/cm): | 525.38 | 525.38 |
| Stop Cubic Rate (N/cm^3): | 162.87 | 162.87 |
| Stop Energy Ratio (%/100): | 0.50 | 0.50 |
| Deflection to Jounce Stop (cm): | 10.16 | 10.16 |
| Stop Linear Rate (N/cm): | 525.38 | 525.38 |
| Stop Cubic Rate (N/cm^3): | 162.87 | 162.87 |
| Stop Energy Ratio (%/100): | 0.50 | 0.50 |
| Roll Steer Const. Coef (deg): | 0.00 | 0.00 |
| Roll Steer Linear Coef (deg/cm): | 0.00 | 0.00 |
| Roll Steer Quadratic Coef (deg/cm): | 0.00 | 0.00 |
| Roll Steer Cubic Coef (deg/cm): | 0.00 | 0.00 |

Camber and Half-track Tables

| Right Side | | | Left Side | | |
|---|---|---|---|---|---|
| Susp Defl (cm) | Camber (deg) | 1/2-track Change (cm) | Susp Defl (cm) | Camber (deg) | 1/2-track Change (cm) |
| -10.16 | 0.50 | 0.00 | -10.16 | 0.50 | 0.00 |
| 0.00 | 0.50 | 0.00 | 0.00 | 0.50 | 0.00 |
| 10.16 | 0.50 | 0.00 | 10.16 | 0.50 | 0.00 |

Tire Information, Second Axle ---

| | Right Side | Left Side |
|---|---|---|
| Tire Name: | Generic | Generic |
| Tire Manufacturer: | Generic | Generic |
| Tire Model: | Generic | Generic |
| Tire Size: | P195/60R15 | P195/60R15 |
| Version No: | es\db\E | es\db\E |
| Unloaded Radius (cm): | 30.75 | 30.75 |
| Init. Radial Stiffness (N/cm/tire): | 2637.99 | 2637.99 |
| 2nd Radial Stiffness (N/cm/tire): | 26379.88 | 26379.88 |
| Defl. @ 2nd Stiffness (cm): | 9.36 | 9.36 |
| Max Deflection (cm): | 11.70 | 11.70 |
| Rebound Energy Ratio (%/100): | 1.00 | 1.00 |
| Spin Inertia (Tire+Whl+Brk, kg-m^2/tire) | 0.89 | 0.89 |
| Steer Inertia (Tire+Whl+Brk, kg-m^2/tire | 0.44 | 0.44 |
| Weight (Tire+Whl+Brk, N/tire): | 182.88 | 182.88 |
| Roll Resistance Const: | 0.01 | 0.01 |
| Roll Resististance Linear Coef (sec/m): | 0.00 | 0.00 |
| Min Fz For Skidmark (N): | 1370.05 | 1370.05 |
| Pneumatic Trail (cm): | -2.19 | -2.19 |
| Lateral Stiffness (N/cm): | 2637.99 | 2637.99 |

| Cornering Stiffness (N/deg/tire): | Right Side | | | Left Side | | |
|---|---|---|---|---|---|---|
| Loads (N): | 2701.4 | 5471.8 | 8210.1 | 2701.4 | 5471.8 | 8210.1 |
| Speeds (m/sec): | 13.4 | | | 13.4 | | |

| | Right Side | | | Left Side | | |
|---|---|---|---|---|---|---|
| Load No.: | 1 | 2 | 3 | 1 | 2 | 3 |
| Speed No. 1: | 778.4 | 778.4 | 778.4 | 778.4 | 778.4 | 778.4 |

| Camber Stiffness (N/deg/tire): | Right Side | | | Left Side | | |
|---|---|---|---|---|---|---|
| Loads (N): | 2727.6 | 5496.7 | 8259.5 | 2727.6 | 5496.7 | 8259.5 |
| Speeds (m/sec): | 13.4 | | | 13.4 | | |
| Load No.: | 1 | 2 | 3 | 1 | 2 | 3 |
| Speed No. 1: | 22.3 | 55.7 | 85.5 | 22.3 | 55.7 | 85.5 |

| Tire Friction Table: | Right Side | | | Left Side | | |
|---|---|---|---|---|---|---|
| Loads (N): | 2740.1 | 5466.9 | 8193.6 | 2740.1 | 5466.9 | 8193.6 |
| Speeds (m/sec): | 13.4 | | | 13.4 | | |
| Speed No. 1, Load No.: | 1 | 2 | 3 | 1 | 2 | 3 |
| Peak Mu: | 1.0500 | 1.0500 | 1.0500 | 1.0500 | 1.0500 | 1.0500 |
| Slide Mu: | 0.7500 | 0.7500 | 0.7500 | 0.7500 | 0.7500 | 0.7500 |
| Slip @ Peak Mu (%/100): | 0.2440 | 0.1680 | 0.1460 | 0.2440 | 0.1680 | 0.1460 |
| Long. Stiffness (N/slip): | 58574.2 | 103123.1 | 184828.1 | 58574.2 | 103123.1 | 184828.1 |

Brake Information, Second Axle ---

| | Right Side | Left Side |
|---|---|---|
| Brake Assembly Type: | Generic Brake | Generic Brake |
| Brake Time Lag (sec): | 0.0000 | 0.0000 |
| Brake Time Rise (sec): | 0.0000 | 0.0000 |
| Pushout Pressure (kPa): | 34.47 | 34.47 |
| Nominal Brake Torque Ratio (N-m/kPa): | 0.30 | 0.30 |
| Brake Proportioning Pressure (kPa): | 1378.95 | 1378.95 |
| Brake Proportioning Ratio: | 0.39 | 0.39 |

## D4: EDSMAC4, w/ aero drag, Vehicle: 1991 Honda-Accord

----- ACCIDENT HISTORY -----

| | time (sec) | X (m) | Y (m) | PSI (deg) | Vtot (km/h) | U (km/h) | V (km/h) | Yaw Vel (deg/sec) |
|---|---|---|---|---|---|---|---|---|
| -Start of Simulation- | | | | | | | | |
| Honda Accord 4-Dr - E | 0.0000 | 0.0 | -30.5 | 0.0 | 99.9 | 99.9 | 0.0 | 0.0 |
| --- At Final/Rest --- | | | | | | | | |
| Honda Accord 4-Dr - E | 6.7760 | 99.7 | -16.9 | 149.9 | 0.0 | 0.0 | 0.0 | 0.0 |

----------DRIVER CONTROL TABLES ------------

Driver Controls for Ford Crown Victoria 4-Dr

Steer Table:

| Time (sec) | R/F (deg) | L/F (deg) | R/R (deg) | L/R (deg) |
|---|---|---|---|---|
| 0.0000 | 0.00 | 0.00 | 0.00 | 0.00 |

Throttle Table:

| Time (sec) | R/F (%/100) | L/F (%/100) | R/R (%/100) | L/R (%/100) |
|---|---|---|---|---|
| 0.0000 | 0.00 | 0.00 | 0.00 | 0.00 |

Brake Table:

| Time (sec) | R/F (N) | L/F (N) | R/R (N) | L/R (N) |
|---|---|---|---|---|
| 0.0000 | -35.41 | -35.41 | -396.34 | -396.34 |

GENERAL ENVIRONMENT DATA

| | |
|---|---|
| Ambient Temperature (Celsius): | 20.00 |
| Ambient Pressure (kPa): | 101.32 |
| Gravity Constant (m/sec^2): | 9.81 |

3-D ENVIRONMENT TERRAIN DATA

| | |
|---|---|
| 3-D Geometry Filename: | (Unknown) |
| Number of Polygons: | 10 |
| GetSurfaceInfo: | From Previous Polygon |
| Minimum Terrain Elevation (m): | 0.00 |
| Maximum Terrain Elevation (m): | 0.00 |

# VEHICLE EVENT DATA

Event Data for Honda Accord 4-Dr - EDSMAC:

Accelerometer Information -- (No Accelerometers)

Event Wheel Data, Wheels & Tires, Front Axle --
Wheel Displacements: (No Displaced Wheels)

Tire Blow-outs: (No Tire Blow-outs)

Event Wheel Data, Second Axle --
Wheel Displacements: (No Displaced Wheels)

Tire Blow-outs: (No Tire Blow-outs)

## GENERAL PROGRAM INFORMATION

| | |
|---|---|
| EDSMAC4 Version No: | 6.60 |

## SIMULATION CONTROLS

| | |
|---|---|
| Max Simulation Time (sec): | 10.0000 |
| Collision Phase dt (sec): | 0.0010 |
| Separation Phase dt (sec): | 0.0010 |
| Trajectory Phase dt (sec): | 0.0010 |
| Output Interval (sec): | 0.0010 |
| Linear Term Vel (km/h): | 0.40 |
| Angular Term Vel (deg/sec): | 5.00 |

-------------------- VEHICLE DATA --------------------

| | |
|---|---|
| Vehicle Name: | Honda Accord 4-Dr - EDSM |
| Vehicle Type: | Passenger Car |
| Vehicle Version Number: | V 5.20 |
| Body Overall Length (cm): | 467.36 |
| Body CG To Front (cm): | 195.23 |
| Body CG To Rear (cm): | -272.13 |
| Body Overall Width (cm): | 172.47 |
| CG Elevation (cm): | 54.00 |
| Roll Couple Dist: | 0.55 |
| Total Weight (N): | 14172.03 |
| Total Mass (kg): | 1443.98 |
| Yaw Inertia Tot (kg-m^2): | 2725.66 |
| Yaw Inertia Sprg (kg-m^2): | 2539.07 |
| 3-D Geometry Filename: | PCHondaAccord924Dr.h3d |
| Number of Vertices: | 0 |
| Number of Damaged Vertices: | 0 |

| | A Stiff (N/cm) | B Stiff (N/cm^2) |
|---|---|---|
| Front End: | 587.7 | 81.5 |
| Right Side: | 430.8 | 59.3 |
| Back End: | 418.6 | 75.8 |
| Left Side: | 430.8 | 59.3 |

----------------- WHEEL AND TIRE DATA ----------------

| Wheels & Tires, Front Axle -- | Right | Left |
|---|---|---|
| Wheel Locn (cm) - x: | 106.00 | 106.00 |
| y: | 73.50 | -73.50 |
| z: | 23.25 | 23.25 |
| Tire Name: | Generic | Generic |
| Tire Size: | P195/60R15 | P195/60R15 |
| Slide Mu (*): | 0.75 | 0.75 |
| Vel Dependence (sec/m): | 0.00000 | 0.00000 |
| Cornering Stiffness (N/deg): | 1005.30 | 1005.30 |

| Second Axle -- | Right | Left |
|---|---|---|
| Wheel Locn (cm) - x: | -166.00 | -166.00 |
| y: | 73.50 | -73.50 |
| z: | 23.25 | 23.25 |
| Tire Name: | Generic | Generic |
| Tire Size: | P195/60R15 | P195/60R15 |
| Slide Mu (*): | 0.75 | 0.75 |
| Vel Dependence (sec/m): | 0.00000 | 0.00000 |
| Cornering Stiffness (N/deg): | 778.44 | 778.44 |

----------------- STEERING SYSTEM DATA ---------------

| | |
|---|---|
| First Axle: | Steerable |
| Steering Gear Ratio (deg/deg): | 16.62 |
| Second Axle: | Not Steerable |